

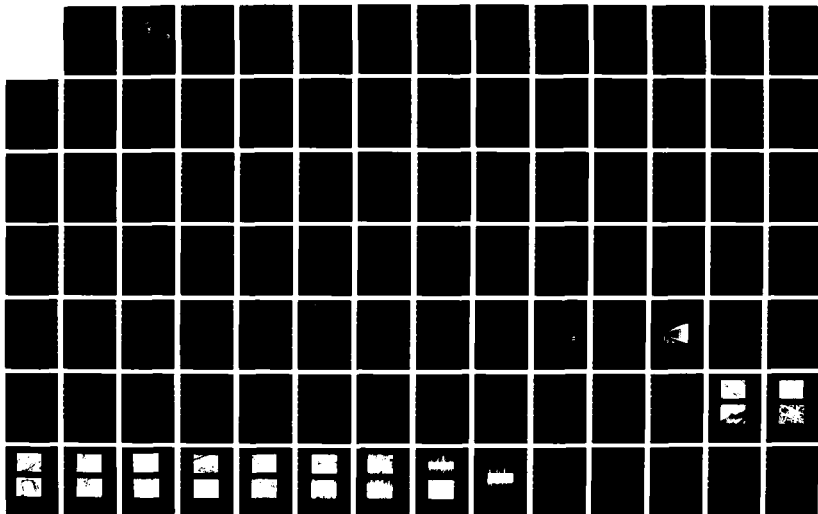
NO-A188 048

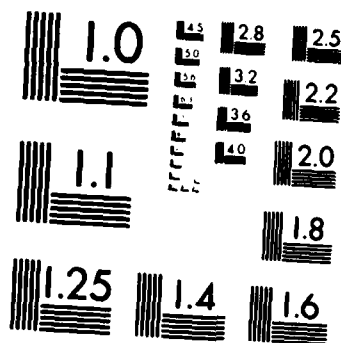
CORROSION PERFORMANCE OF HIGH DAMPING ALLOYS IN 35%
SODIUM CHLORIDE ENVIRONMENT(U) NAVAL POSTGRADUATE
SCHOOL MONTEREY CA 5 AKHTAR SEP 87

1/2

UNCLASSIFIED

F/G 11/6.1 NL





MICROCOPY RESOLUTION TEST CHART
NATIONAL BUREAU OF STANDARDS 1963 A

2

NAVAL POSTGRADUATE SCHOOL

Monterey, California

DTIC FILE COPY

AD-A188 048



THESIS

DTIC
SELECTED
JAN 26 1988
S E D

CORROSION PERFORMANCE OF HIGH DAMPING
ALLOYS IN 3.5% SODIUM CHLORIDE ENVIRONMENT

by

Saleem Akhtar

September 1987

Thesis Advisor:

Jeff Perkins

Approved for Public release; distribution is unlimited

88 1 21 020

UNCLASSIFIED

SECURITY CLASSIFICATION OF THIS PAGE

REPORT DOCUMENTATION PAGE

1a REPORT SECURITY CLASSIFICATION Unclassified			1b RESTRICTIVE MARKINGS		
2a SECURITY CLASSIFICATION AUTHORITY			3 DISTRIBUTION/AVAILABILITY OF REPORT Approved for public release; Distribution is unlimited		
2b DECLASSIFICATION/DOWNGRADING SCHEDULE					
4 PERFORMING ORGANIZATION REPORT NUMBER(S)			5 MONITORING ORGANIZATION REPORT NUMBER(S)		
6a NAME OF PERFORMING ORGANIZATION Naval Postgraduate School		6b OFFICE SYMBOL (if applicable) 69	7a NAME OF MONITORING ORGANIZATION Naval Postgraduate School		
6c ADDRESS (City, State, and ZIP Code) Monterey, CA 93943-5000			7b ADDRESS (City, State, and ZIP Code) Monterey, CA 93943-5000		
8a NAME OF FUNDING/SPONSORING ORGANIZATION		8b OFFICE SYMBOL (if applicable)	9 PROCUREMENT INSTRUMENT IDENTIFICATION NUMBER		
8c ADDRESS (City, State, and ZIP Code)			10 SOURCE OF FUNDING NUMBERS		
			PROGRAM ELEMENT NO	PROJECT NO	TASK NO
			WORK UNIT ACCESSION NO		
11 TITLE (Include Security Classification) Corrosion Performance of High Damping Alloys in 3.5% Sodium Chloride Solution					
12 PERSONAL AUTHOR(S) SALEEM AKHTAR					
13a TYPE OF REPORT Masters Thesis		13b TIME COVERED FROM TO		14 DATE OF REPORT (Year, Month, Day) September 1987	
15 PAGE COUNT 113					
16 SUPPLEMENTARY NOTATION					
COSATI CODES			18 SUBJECT TERMS (Continue on reverse if necessary and identify by block number)		
FIELD	GROUP	SUB-GROUP	Corrosion, High Damping Alloys, Electrochemical Technique, Sea Exposure, Scanning Electron Microscopy (SEM)		
19 ABSTRACT (Continue on reverse if necessary and identify by block number)					
<p>The electrochemical nature of corrosion provides a means of determining an almost instantaneous corrosion rate. Corrosion rate and the nature of corrosion attack were investigated for several high damping alloys based on the Cu-Mn, Fe-Cr-Al, Fe-Cr-Mo, and Cu-Zn systems in 3.5% NaCl solution.</p> <p>The results of Potentiodynamic polarization and polarization resistance measurements were compared with the results of actual sea exposures. A zero resistance ammeter technique was used to measure the galvanic currents between galvanically coupled metals. The magnitude of the galvanic current provide an indication of the severity of galvanic corrosion which occurs in a 3.5% NaCl environment.</p> <p>Scanning electron microscopy (SEM) was used to determine the nature of corrosion attack and the extent of film formation on the surface of each corroding alloy.</p>					
20 DISTRIBUTION/AVAILABILITY OF ABSTRACT <input checked="" type="checkbox"/> UNCLASSIFIED/UNLIMITED <input type="checkbox"/> SAME AS RPT <input type="checkbox"/> OTIC USERS			21 ABSTRACT SECURITY CLASSIFICATION Unclassified		
22a NAME OF RESPONSIBLE INDIVIDUAL Professor Jeff Perkins			22b TELEPHONE (Include Area Code) 408-646-2216		22c OFFICE SYMBOL 69Bs

UNCLASSIFIED

SECURITY CLASSIFICATION OF THIS PAGE (When Data Entered)

19. ABSTRACT (CONT)

Results from Laboratory and actual sea exposures showed that the Fe-Cr-Al and Fe-Cr-Mo high damping alloys experienced severe localized corrosion and pitting. 630 Bronze and Cu-Mn-Al based alloys indicate low to moderate corrosion rates.

S. N 0102- LF- 014- 6601

UNCLASSIFIED

SECURITY CLASSIFICATION OF THIS PAGE (When Data Entered)

Approved for public release; distribution is unlimited.

Corrosion performance
of
High damping alloys in 3.5% sodium chloride Solution

by

Saleem Akhtar
Lieutenant Commander, Pakistan Navy
B.E., University of Karachi, 1977

Submitted in partial fulfillment of the
requirements for the degree of



MASTER OF SCIENCE IN MECHANICAL ENGINEERING

from the

NAVAL POSTGRADUATE SCHOOL
September 1987

Accession For	
NTIS GRA&I	<input checked="" type="checkbox"/>
DTIC TAB	<input type="checkbox"/>
Unannounced	<input type="checkbox"/>
Justification	
By _____	
Distribution/	
Availability Codes	
Avail and/or	
Dist	Special
A-1	

Author:

Saleem Akhtar

Saleem Akhtar

Approved by:

Jeff Perkins

Jeff Perkins, Thesis Advisor

A.J. Healey

A.J. Healey, Chairman,
Department of Mechanical Engineering

Gordon E. Schacher

Gordon E. Schacher,
Dean of Science and Engineering

ABSTRACT

The electrochemical nature of corrosion provides a means of determining an almost instantaneous corrosion rate. Corrosion rate and the nature of corrosion attack were investigated for several high damping alloys based on the Cu-Mn, Fe-Cr-Al, Fe-Cr-Mo, and Cu-Zn systems in 3.5% NaCl solution. The results of Potentiodynamic polarization and polarization resistance measurements were compared with the results of actual sea exposures. A zero resistance ammeter technique was used to measure the galvanic currents between galvanically coupled metals. The magnitude of the galvanic current provide an indication of the severity of galvanic corrosion which occurs in a 3.5% NaCl environment. Scanning electron microscopy (SEM) was used to determine the nature of corrosive attack and the extent of film formation on the surface of each corroding alloy. Results from Laboratory and actual sea exposures showed that the Fe-Cr-Al and Fe-Cr-Mo high damping alloys experienced severe localized corrosion and pitting. 630 Bronze and Cu-Mn-Al based alloys indicate low to moderate corrosion rates.

TABLE OF CONTENTS

I. INTRODUCTION	18
II. BASIC CORROSION THEORY - A REVIEW OF EXPERIMENTAL TECHNIQUES	20
A. POTENTIODYNAMIC POLARIZATION	20
B. POLARIZATION RESISTANCE	24
C. OTHER METHODS FOR ASSESSING CORROSION DAMAGE	25
D. DETERMINATION OF TAFEL CONSTANTS	26
E. GALVANIC CORROSION	28
III. EXPERIMENTAL EQUIPMENT AND PROCEDURES	31
A. EXPERIMENTAL EQUIPMENT	31
1. The Corrosion Cell	31
2. Galvanic Set Up	31
3. The Potentiostat	32
4. The Processor	32
5. The Model 351 Corrosion Measurement System	32
B. EXPERIMENTAL PROCEDURES FOR SYNTHETIC SEAWATER EXPOSURES	33
C. SAMPLE PREPARATION	34
D. TESTED MATERIALS	35

E. EXPERIMENTAL PARAMETERS	36
F. SCANNING ELECTRON MICROSCOPY	37
G. EXPERIMENTAL PROCEDURES FOR NATURAL SEAWATER EXPOSURES	37
IV. RESULTS AND DISCUSSION	39
A. SINGLE METAL CORROSION.....	39
1. 7075 Aluminum	39
2. 304 Stainless Steel	40
3. Fe-Cr-Mo	42
4. Fe-Cr-Al	43
5. Cu-Mn-Al-Fe-Ni	45
6. Cu-Mn-Al	46
7. 630 Series Bronze	47
B. GALVANIC COUPLING	48
1. Select Galvanic Couples	49
2. Galvanic Series of Selected High Damping and Baseline Alloys in Quiescent 3.5% Sodium Chloride Solution	54
V. CONCLUSIONS AND RECOMMENDATIONS	55
APPENDIX A: FIGURES	104
APPENDIX B: PREPARATION OF 3.5% CHLORIDE SOLUTION	105

APPENDIX C: STANDARD OPERATING PROCEDURES

FOR THE MODEL 351 CORROSION

MEASUREMENT SYSTEM	107
LIST OF REFERENCES	109
INITIAL DISTRIBUTION LIST	111

LIST OF TABLES

1. COMPARISON OF CORROSION RATES OF THE HIGH
DAMPING ALLOYS IN 3.5% SODIUM CHLORIDE,
NATURAL SEA WATER AND SYNTHETIC SEA WATER
ENVIRONMENTS104

LIST OF FIGURES

1. Potentiodynamic Polirization plot of 430 stainless steel in H_2SO_4	56
2. Theoretical potentiodynamic polarization plot showing anodic and cathodic Tafel regions	56
3. Polarization resistance plot	57
4. Best fit method for determining Tafel Constants	57
5. Basic zero resistance ammeter circuit	58
6. Schematic circuit for use of a potentiostat as a zero resitance ammeter	58
7. Working electrode sample holder	59
8. Standard K47 corrosion cell	60
9. Galvanic corrosion cell arrangement	61
10. Format for a Potentiodynamic polarization experiment	62
11. Basic system installation for potentiodynamic polarization and polarization resistance experiment	63
12. Galvanic corrosion set up	64
13. Low velocity sea water trough	65
14. Potentiodynamic polarization plot for 7074 Aluminum in 3.5% Sodium Chloride solution	66

15. Polarization resistance plot for 7075	
Aluminum in 3.5% Sodium Chloride solution	67
16. Potentiodynamic polarization plot for 630	
Bronze in 3.5% Sodium Chloride solution	68
17. Polarization resistance plot for 630	
Bronze in 3.5% Sodium Chloride solution	69
18. Potentiodynamic polarization plot for	
Fe-Cr-Mo in 3.5% Sodium Chloride solution	70
19. Polarization resistance plot for	
Fe-Cr-Mo in 3.5% Sodium Chloride solution	71
20. Potentiodynamic polarization plot for	
Fe-Cr-Al in 3.5% Sodium Chloride solution	72
21. Polarization resistance plot for	
Fe-Cr-Al in 3.5% Sodium Chloride solution	73
22. Potentiodynamic polarization plot for	
Cu-Mn-Al (INCRAMUTE) in 3.5% Sodium	
Chloride solution	74
23. Polarization resistance plot for	
Cu-Mn-Al (INCRAMUTE) in 3.5% Sodium	
Chloride solution	75
24. Potentiodynamic polarization plot for 304	
Stainless Steel in 3.5% Sodium Chloride	
solution	76
25. Polarization resistance plot for 304	
Stainless Steel in 3.5% Sodium Chloride	
solution	77

26. Potentiodynamic polarization plot for Cu-Mn-Al-Fe-Ni (SONOSTON) in 3.5% Sodium Chloride solution	78
27. Polarization resistance plot for Cu-Mn-Al-Fe-Ni (SONOSTON) in 3.5% Sodium Chloride solution	79
28. As-machined surface of 7075 Aluminum prior to sea water exposure at LaQue Center	80
29. Corroded surface of 7075 Aluminum after 150 days exposure at LaQue Center	80
30. As-machined surface of 630 Bronze prior to sea water exposure at LaQue Center	81
31. Corroded surface of 630 Bronze after 150 days exposure at LaQue Center	81
32. As-machined surface of Fe-Cr-Mo prior to sea water exposure at LaQue Center	82
33. Corroded surface of Fe-Cr-Mo after 150 days exposure at LaQue Center	82
34. As machined surface of Fe-Cr-Al prior to sea water exposure at LaQue Center	83
35. Corroded Surface of Fe-Cr-Al after 150 days exposure at LaQue Center	83
36. As machined surface of Cu-Mn-Al (INCRAMUTE) prior to sea water exposure at LaQue Center	84
37. Corroded Surface of Cu-Mn-Al (INCRAMUTE) after 150 days exposure at LaQue Center	84

38. As machined surface of 304 Stainless Steel prior to sea water exposure at LaQue Center	85
39. Corroded Surface of 304 Stainless Steel after 150 days exposure at LaQue Center	85
40. As machined surface of Cu-Mn-Al-Fe-Ni (Sonoston) prior to sea water exposure at LaQue Center.....	86
41. Corroded Surface of Cu-Mn-Al-Fe-Ni (Sonoston) after 150 days exposure at LaQue Center	86
42. Surface appearance of 7075 Aluminum . after 150 days exposure at LaQue Center	87
43. Surface appearance of 630 Bronze after 150 days exposure at LaQue Center	87
44. Surface appearance of Fe-Cr-Mo after 150 days exposure at LaQue Center	88
45. Surface appearance of Fe-Cr-Al after 150 days exposure at LaQue Center	88
46. Surface appearance of Cu-Mn-Al (INCRAMUTE) after 150 days exposure at LaQue Center	89
47. Surface appearance of 304 Stainless Steel after 150 days exposure at LaQue Center	89
48. Surface appearance of Cu-Mn-Al-Fe-Ni (Sonoston) after 150 days exposure at LaQue Center	90

49. Galvanic current and potential Vs time curves for 7075 Aluminum coupled with 670 Bronze in 3.5% Sodium Chloride solution	91
50. Galvanic current and potential Vs time curves for 7075 Aluminum coupled with Ingramite in 3.5% Sodium Chloride solution	92
51. Galvanic current and potential Vs time curves for 7075 Aluminum coupled with Sonoston in 3.5% Sodium Chloride solution	93
52. Galvanic current and potential Vs time curves for 7075 Aluminum coupled with Fe-Cr-Mo in 3.5% Sodium Chloride solution	94
53. Galvanic current and potential Vs time curves for 7075 Aluminum coupled with 304 Stainless Steel in 3.5% Sodium Chloride solution	95
54. Galvanic current and potential Vs time curves for 7075 Aluminum coupled with Fe-Cr-Al in 3.5% Sodium Chloride solution	96
55. Galvanic current and potential Vs time curves for 304 Stainless Steel coupled with Sonoston in 3.5% Sodium Chloride solution	97

56. Galvanic current and potential Vs time curves for 304 Stainless Steel coupled with 630 Bronze in 3.5% Sodium Chloride solution	98
57. Galvanic current and potential Vs time curves for 304 Stainless Steel coupled with Incramute in 3.5% Sodium Chloride solution	99
58. Galvanic current and potential Vs time curves for 304 Stainless Steel coupled with Fe-Cr-Al in 3.5% Sodium Chloride solution	100
59. Galvanic current and potential Vs time curves for 304 Stainless Steel coupled with Fe-Cr-Mo in 3.5% Sodium Chloride solution	101
60. Summary of results of coupling 7075 Aluminum with rest of the alloys	102
61. Summary of results of coupling 304 Stainless Steel with rest of the alloys	103

LIST OF SYMBOLS AND ABBREVIATIONS

cm	centimeter
cm ²	centimeter squared
C.R.	corrosion rate
E _{corr}	Corrosion potential of a single metal
E _{couple}	corrosion potential of a metal couple
E.W.	equivalent weight
g	gram
i _{corr}	corrosion current density of a single metal
i _{couple}	corrosion current density of a metal couple
kg	kilogram
L(1)	liter
LPR	Linear Polarization Resistance
m	meter
ml	milliliter
mm	millimeter
mpy	mils per year
mV	millivolt
uA	microampere
PAB	Princeton Applied Research
PDP	potentiodynamic polarization
R _{mpy}	corrosion rate in mils per year
SCE	saturated calomel electrode

SEM	scanning electron microscope/microscopy
V	volt
X	magnification

ACKNOWLEDGEMENTS

The author wishes to express his appreciation to all those whose assistance and encouragement made this investigation possible. Special thanks are due to Professor A.J. Perkins for guidance and encouragement throughout this investigation; also to T.F. Kellogg for assistance in developing techniques and providing the necessary guidance in the use of laboratory equipment; to Pakistan Navy for giving me the opportunity to study at the Naval Postgraduate School; and to my wife Shahnaz, without her support and encouragement this work would not have been possible.

I. INTRODUCTION

High damping alloys are used in various equipment and structures which are subjected to corrosive attack. The prediction of their performance in a corrosive environment can be made using standard laboratory techniques. These laboratory results can then be compared with the results achieved in natural environment. The purpose of the present research is to present the results and experimental procedures used to obtain corrosion rates and corrosion characteristics of high damping alloys in a marine environment.

A number of experimental techniques were applied, resulting in the determination of representative corrosion rates and anticipated modes of corrosive attack. Potentiodynamic Polarization and Linear Polarization (performed on the Princeton Applied Research model 351 Corrosion Measurement System) were utilized to determine the simple metal corrosion rates of these alloys. A galvanic corrosion technique was then used to measure the current between galvanically coupled metals, in order to provide an indication of the severity of galvanic corrosion in various cases. These techniques were also used for the determination of a galvanic series for both high damping and common baseline alloys in quiescent, 3.5% NaCl solution.

Results from concurrent sea exposure of the alloys (conducted at The La Que Centre for Corrosion Technology, Wright Sville Beach, N.C.) were compared with the laboratory results to better characterize the corrosion behavior of the high damping alloys for in-service marine applications.

Scanning electron microscopy was used following laboratory experimentation and sea exposures to analyze the modes of surface attack experienced by each alloy.

A brief summary of applicable corrosion/electrochemical theory and analytical expressions are presented prior to discussing procedures and results.

II. BASIC CORROSION THEORY - A REVIEW OF EXPERIMENTAL TECHNIQUES

Many corrosion processes can be explained in terms of electrochemical reactions. Measurements of current and potential in a controlled environment can provide information regarding corrosion rates, film formation and pitting tendencies.

A. THE POTENTIODYNAMIC POLARIZATION TECHNIQUE

Potentiodynamic Polarization is an electrochemical technique in which the potential of the metal sample of interest is continuously scanned in the anodic direction. Potential values achieved during the scan are plotted against the current density (current per surface area). As the specimen is scanned anodically, an oxide coating may form on the surface of the specimen. Potentiodynamic polarization measurements yield corrosion characteristics of an alloy in a given aqueous solution.

When a metal specimen is immersed in a corrosive medium, the sample assumes a potential relative to a reference electrode. This relative potential is termed the corrosion potential of the specimen, E_{corr} . At E_{corr} , simultaneous anodic and cathodic reactions are occurring at the surface. The specimen is at an equilibrium condition and no net

external current is passed. The rate of oxidation and reduction are equal at E_{corr} .

An example of a potentiodynamic polarization experiment is shown in Figure 1. Region A exhibits typical active corrosion of the sample. At B, a continued increase in applied potential results in a decreasing current density, corresponding to a decreased rate of corrosion. This occurs at the onset of film formation. Region C is characterized by decreasing current density with further increase in potential, as the passivating film develops and more fully covers the surface of the sample. Region D shows minimal changes in current density as the potential is increased; this is designated as the Passivation Region. A further increase in potential may result in an increase in current density and a breakdown of the passivating film, so that Region E is designated as the Transpassive Region and is usually characterized by pitting of the sample.

Corrosion rates can be obtained by extrapolation of the linear (Tafel) regions (near E_{corr}) for either the anodic or cathodic branches of the potentiodynamic polarization plot, or both. For example, Figure 2 shows extrapolations of the Tafel regions intercepting at E_{corr} . The value of current density at the intercept is defined as i_{corr} , which is directly related to corrosion rate calculations. The Tafel regions generally start ± 50 mv from E_{corr} and may extend from 1 to 3 decades in length on the current density axis.

However in many experiments, the Tafel region can be extremely limited, and determination of slopes in the Tafel region (Ba, Bc) can prove extremely difficult. This point will be addressed later in more detail. Once a value of i_{corr} is determined, corrosion rate calculations can be made using Faraday's Law:

$$Q = \frac{nFW}{M} \quad (1)$$

where Q = Coulombs

n = number of electrons involved in the electrochemical reaction

F = the Faraday, 96,487 coulombs

W = weight of the atomic species

M = the molecular weight

Since M/n is defined as the Equivalent Weight of the sample, and Q is equal to current multiplied by time, the following relationship holds:

$$\frac{W}{t} = \frac{(E.W)}{F} i_{corr} \quad (2)$$

where W/t is the corrosion rate in grams per second.

Corrosion rate is typically expressed in milliinches per year (mils per year). Dividing Equation (2) by the sample area and density and using appropriate conversions results in the following:

$$\text{C.R (mpy)} = \frac{0.13 \text{ } i_{\text{corr}} (\text{E.W})}{d} \quad (3)$$

where i_{corr} = the corrosion current density (A/cm²)

E.W. = the Equivalent Weight of the material (g)

d = the density of the sample in g/cm³

C.R. = corrosion rate in mils per year (mpy)

Equation (3) can be used to calculate the corrosion rate of a given alloy in mils per year.

Advantages of the potentiodynamic Polarization method are:-

1. Readily apparent observation of film formation/passivation.
2. Determination of the rate of corrosion.
3. Relatively short period of time required for completion of the experiment.

Disadvantages of this method are:

1. Tafel slopes may be very difficult to determine.
2. Scanning the sample deteriorates the sample's surface preventing further experimentation using the same sample.

B. POLARIZATION RESISTANCE TECHNIQUE

The Polarization Resistance Technique is a rapid method for determining the corrosion rate of a tested material. The experimental apparatus is identical to that used for the Potentiodynamic Polarization technique. However, potential scanning of the sample is only performed over a small range (± 25 mV) near E_{corr} . In this region of scanning, the applied current density is a linear function of the applied potential. Current density and potential are both plotted on a linear scale as shown in Figure 3.

The value for i_{corr} is directly related to the slope of the Polarization plot by the Stearn-Geary equation:

$$P.R. = \frac{B_a B_c}{2.3(i_{corr})(B_a + B_c)} \quad (4)$$

where P.R. = slope of the Polarization Resistance plot in
Ohms

B_a, B_c = Tafel slopes in Volts/Decade

i_{corr} = corrosion current density in μA .

Rearranging Equation (4) yields:

$$i_{corr} = \frac{B_a B_c}{2.3(B_a + B_c)} \cdot \frac{1}{P.R.} \quad (5)$$

Solving for i_{corr} using Equation (5) allows for direct substitution into Equation (3) for determination of

corrosion rate. The major advantage of this method is the speed of determination of a sample's corrosion rate. The Polarization Resistance experiment can be performed in a matter of only several minutes and is referred to as method 2 in section IV.

C. OTHER METHODS FOR ASSESSING CORROSION DAMAGE

Direct weight loss measured on a corroded specimen is another commonly used technique for determining corrosion rates. This method is extremely simple in nature and can be performed with relatively unsophisticated equipment. Concurrent corrosion experiments performed at the La Que Centre as part of the present research program utilized direct weight loss measurements for determination of corrosion rates.

In order to achieve the most consistent results, weight loss measurements should be made on samples of equal size and geometry and exposed to the corrosive medium for an identical period of time. The corrosion rate can then be determined.

Even though this method is quickly and easily accomplished, there are several disadvantages, including:

1. Corrosion rate determinations assume that all weight loss has occurred from general corrosion; localized modes are not considered.

2. This method assumes that the material has not been internally attacked by other forms of corrosion such as dealloying, intergranular corrosion, etc.
3. Extreme care is required when the corrosion product is removed from the sample. Some of the base metal may accidentally be removed, leading to inaccurate results.

Pit depth determination is another valuable method for assessing corrosion damage. The LaQue Center also performed this analysis when applicable. If the pitting is broad and shallow, pit depth calipers can be used.

Deeper, narrower pits require depth determination by means of cross-sectional microscopy.

D. DETERMINATION OF TAFEL CONSTANTS

The exact determination of the Tafel slopes is extremely difficult in some cases, depending upon the material being tested and the corrosive medium. The extent of Tafel regions are directly influenced by several factors, including concentration polarization, multiple reduction processes, active-to-passive transitions, and the IR drop related to the conductivity of the electrolyte. Pourbaix has shown that using a value of 0.1 volts/Decade for both Tafel constructs yields a corrosion rate within a factor of 2 to 3. In the present work, two methods were utilized for calculation of corrosion rates and a different approach was

made for determination of Tafel slopes, called the Best Fit method.

Method 1: "Best Fit" method with PDP curves

This method is useful when at least one of the Tafel region is apparent. As shown in Figure 4, a straight line is drawn parallel to the current density axis through E_{corr} . Both the Tafel slopes have to meet somewhere on this line. In this example, a tangent is drawn on the anodic curve, which has distinct Tafel region. The intersection of this Tangent (A) with the horizontal line through E_{corr} is represented by point B. This point signifies that i_{corr} is located in close vicinity to this point. If the cathodic curve exhibit Tafel region a similar approach can be used as described above. However, in the absence of such a region, a tangent is drawn to the cathodic curve such that it passes in close proximity to point B and also ensures that angles C and D are equal. Once this is done, the tangents can be changed slightly so that they pass through just one point, which locates i_{corr} . The corrosion rate is then determined using equation (3). This method has been successfully used in the present work.

Method 2: Tafel Slopes from "Best Fit" method and LPM Data

The Tafel constants obtained from the Best Fit method are then used in the Polarization resistance technique, which provides further values for i_{corr} and corrosion rate (mpy).

E. GALVANIC CORROSION

In this technique, one measures the voltage/current characteristics of a system consisting of two dissimilar metals immersed in a solution. In principle, the two metals may even be in two different solutions which are electrically connected by a salt bridge. Thus, galvanic corrosion measurements normally entail use of a different cell than that used with other electrochemical techniques for the measurement of corrosion.

Measurement of currents between galvanically coupled metals is based on zero resistance ammeter techniques. The basic zero resistance ammeter circuit, which has been extensively used, is shown in Figure 5. The galvanic current is measured by an ammeter, A, by adjusting the voltage, E, or resistance, R, so that the potential difference between the two elements is zero as indicated by the electrometer, V. Since short circuiting in a galvanic couple is indicated by zero potential drop, this current is the true short circuit current. For continuous recording of galvanic currents, the basic circuit is simplified to include a decade resistance box adjusted so that a recorder, set to 1 millivolt full scale, indicates the potential between the two elements. The galvanic current is calculated knowing the resistance and the potential.

The magnitude of the galvanic current provides an indication of the severity of galvanic corrosion which occurs in the specific 3.5% sodium chloride environment. More recent developments include the use of potentiostats incorporating the operational amplifier circuitry. In the arrangement in Figure 6, the control potential of the potentiostat is set to zero volts. One member of the galvanic couple is connected to the working electrode terminal while the other is connected to the reference electrode terminal. The auxiliary electrode terminal is connected directly to the reference electrode terminal whereby the galvanic current is indicated directly by the potentiostat current meter, or, it is connected through an external feed back resistor (R_f in Figure) and the galvanic current is measured by a voltmeter between the auxiliary and the working electrode terminals. A null balance is thus maintained by means of the Potentiostat solid state operational amplifier circuit.

The measured galvanic current is not always a measure of the true corrosion current, because it is the algebraic sum of the currents due to anodic and cathodic reactions. When cathodic currents are appreciable at the mixed potential of the galvanic couple, the measured galvanic current will be significantly lower than the true corrosion current. Thus, large differences between the true corrosion rate calculated

by weight loss and the rate obtained by galvanic current measurements may be observed.

The Model 351 Potentiostat can be made to function primarily as a zero resistance ammeter during galvanic corrosion measurements. We are only required to control the total time over which measurements are taken. While the run is in progress, the galvanic couple potential with respect to the reference electrode and the short circuit current are displayed on the screen. Two separate plots are produced, voltage vs.time and current vs.time.

III. EXPERIMENTAL EQUIPMENT AND PROCEDURES

A. EXPERIMENTAL EQUIPMENT

The key to producing consistent polarization diagrams in this work proved to be the use of a rigidly standardized experimental procedure. With the exception of the potential ranges scanned versus E_{corr} , the methodology for performing the polarization experiments was identical for each alloy tested.

1. The Corrosion Cell

The basic PAR Model K47 corrosion cell consists of a multi-port flask, 2 carbar counter electrodes, a working electrode with a threaded tip for sample attachment (Figure 7), and the Saturated Calomel Reference Electrode. Figure 8 shows an actual view of the corrosion cell.

2. The Corrosion Cell (Galvanic Corrosion)

The Galvanic Corrosion measurements involve the use of two metal "working" electrodes, therefore, the connections are made differently to basic K47 corrosion cell. The cell consists of the multi-port flask, two working electrodes with threaded tips for sample attachment (Figure 7), and the saturated Calomel Reference electrode. Figure 9 shows an actual view of the corrosion cell.

3. The Potentiostat

The PAR Model 272/273 Potentiostat was used throughout this research. The Potentiostat processes the potentials and currents experienced by the operating corrosion cell to allow for data collection and graphical plotting.

4. The Processor

The PAR Model 1000 Processor/computer receives input of the potential and current values from the Potentiostat, processes the data, and generates the polarization plots.

The Processor permits an input of customized test procedures which may be saved for later recall.

5. The Model 351 Corrosion Measurement System

The PAR Model 351 System couples the Model K47 Corrosion Cell, Model 272/273 Potentiostat, the Model 1000 Processor, and a plotter to achieve a versatile, easy-to-use system suited to perform a variety of corrosion experiments. The touch screen format allows rapid modification of experimental procedures. Figure 10 shows a typical format for a Potentiodynamic Polarization experiment. Figure 11 shows the basic system installation for performance of corrosion experiments.

The Model 351 Corrosion measurement System can also process the data from a Potentiodynamic Polarization experiment to obtain Tafel constants. However, the programming used to perform this calculation is inadequate

for determination of the true Tafel regions. As a result, hand calculations were utilized by the author to determine Tafel constants, i_{corr} , and corrosion rates.

Basic operating procedures for the Model 351 system are listed in Appendix B.

B. EXPERIMENTAL PROCEDURES

ASTM standard testing procedures were utilized for conducting polarization experiments. Prior to performing an experiment, all components of the corrosion cell were thoroughly cleaned and dried. A magnetic stirrer was placed in the corrosion cell after filling with approximately 800 ml of 3.5% Sodium Chloride solution.

For the Potentiodynamic technique, the carbar counter electrodes, working electrode with the attached sample and the saturated Calomel reference electrode (SCE) were then inserted as shown in Figure 8. The working distance between the tip of the reference electrode and the sample was adjusted to 2 mm. The electrodes were connected to the Potentiostat via the electrometer as shown in Figure 11. Sample identification, area, density, equivalent weight, scan rate and delay time of on hour duration was then entered and experiment was started, data recorded and Polarization plots generated.

In the case of linear Polarization technique, the cell connection are similar to potentiodynamic, polarization

except that the values of both the Tafel constants, obtained from the potentiodynamic curve are also entered in addition to other data. The experiment is then started and polarization resistance thus obtained is utilized to calculate i_{corr} and corrosion rate.

In Galvanic corrosion, the working electrodes with attached samples and saturated Calomel reference electrode (SCE) are inserted in the cell and connected as shown in Figure 12. The working electrode sample which is expected to be anode is kept at a distance of 2mm from reference electrode tip. The sample identification, run time and smoothing is then entered and the experiment started. On completion of the experiment the data for both galvanic current and galvanic potential Vs time is recorded.

C. SAMPLE PREPARATION

The alloys to be studied were originally provided in various forms (bars, plates, rods, etc...). Most of the alloys were machined into 9.55 mm diameter by 9.55 mm height right circular cylinders and threaded for attachment to the working electrode sample holder shown in Figure 7.

After machining, the samples were always stored in a dessicator during inactive periods. Prior to immersion in the corrosion cell, each sample was weighed and measured after thorough sanding with fine sandpaper. This ensured

that each sample would have a freshly prepared surface, free of any surface oxidation, prior to experimentation.

D. TESTED MATERIALS

Four high damping alloys and three baseline steel, aluminum and copper alloys were examined during this research. The nominal compositions of the high damping alloys are as follows:

Ingramite	58.0% Cu, 40.0% Mn, 2.0% Al
Sonoston	37.0% Cu, 54.25% Mn, 4.25% Al, 3.0% Fe, 1.5% Ni
Fe-Cr-Mo	85.43% Fe, 11.65% Cr, 2.92% Mo
Fe-Cr-Al	85.51% Fe, 11.60% Cr, 2.89% Al

The nominal chemical composition of the baseline alloys were as follows:

304 Stainless Steel	71.92% Fe, 18.5% Cr, 9.5% Ni, .08% C (max)
7075 Aluminum	90% Al, 2.5% Mg, 1.6% Cu, 5.6% Zn, .30% Cr
630 Series Bronze	79.1% Cu, .12% Zn, .032% Sn, .021% Si, 1.4% Mn, 2.76% Fe, 5.35% Ni, 10.9% Al

E. EXPERIMENTAL PARAMETERS

Potentiodynamic Polarization, Polarization Resistance and Galvanic Corrosion experiments were conducted as part of this research. All tests were conducted in 3.5% Sodium chloride solution (Appendix A). The following experimental parameters were used during testing:

1. Potentiodynamic Polarization Technique

a. Scanning Values

1. Final Potential -- Typically + 750 mV vs Ecorr
2. Initial Potential -- Typically - 600 mV vs Ecorr
3. Scanning Rate -- 0.5 mV per second

b. Material Characteristics

1. Equivalent Weight -- Calculated for each specimen
2. Surface Area -- Calculated for each specimen
3. Density -- Calculated for each specimen

2. Polarization Resistance Technique

a. Scanning Values

1. Final Potential -- + 25 mV vs Ecorr
2. Initial Potential -- - 25 mV vs Ecorr
3. Scanning Rate -- 1 mV per second

b. Material Characteristics -- same as previous method

3. Galvanic Corrosion Technique

a. Run time -- About 14 hours

During all experimentation, corrosion cell temperatures were maintained at 21.5 ± 0.5 degrees C.

F. SCANNING ELECTRON MICROSCOPY

The Cambridge Model S200 Scanning Electron Microscope (SEM) was used to determine the nature of corrosive attack and the extent of film formation on the surface of each alloy. Photographs of the original as-machined samples, samples experimentally exposed in synthetic seawater, and samples exposed in natural seawater at the La Que Centre were examined. In general, machined samples were photographed at 1000x while the corroded samples were studied at magnifications up to 2000x. Prior to SEM photography, corroded samples were brushed to remove corrosion products, acid cleaned, brushed with a soap powder and pumice mixture, water rinsed, alcohol rinsed, blown dry with a hot air blower, cooled to room temperature.

G. EXPERIMENTAL PROCEDURES FOR NATURAL SEAWATER EXPOSURES

Concurrent natural seawater exposures were conducted at the La Que Centre. Specimens of the high damping alloys and baseline steel and aluminum alloys were exposed to ambient temperature, low flow, filtered seawater in accordance with ANSI/ASTM Standard G 52 -76 ("Standard Recommended Practice

for Conducting Surface Seawater Exposure Tests on Metals and Alloys"). Prior to immersion of the samples, nonofilament fishing line was attached and the specimens were degreased, lightly brushed, rinsed and dried. The specimens were allowed to cool to ambient temperature prior to weighing. Each specimen was suspended on a support bar and immersed. The 7075 Aluminum samples were exposed in a separate trough to prevent attack from copper-ions emanating from the copper-based alloys. A continuous supply of uncontaminated, full strength seawater at a nominal velocity of .3 m/s was maintained. During the exposure in the low velocity seawater trough (Figure 13), pH, temperature, salinity, and dissolved Oxygen content were monitored. After an exposure period of 150 days, 3 to 4 samples of each alloy were removed from the seawater trough. The corrosion product was removed from each of the samples and corrosion rates and surface characteristics were recorded. One sample of each alloy was returned in its corroded state to allow for subsequent SEM analysis.

IV. RESULTS AND DISCUSSION

A. SINGLE METAL CORROSION

A detailed summary of these results is shown in table [1].

1. 7075 Aluminum

The Electrochemical results for 7075 Aluminum samples are shown in Figure [14] and [15]. The surface appearances of sea water exposed samples are shown in Figure [42]. The PDP plot and the LPM plot yield the following results:

Method	Ba (V/Decade)	Bc (V/Decade)	icorr (A/cm ²)	R(mpy)
1	0.01	2.36	7.406	3.11
2	0.01	2.36	11.70	5.6
AVG				4.355

Direct weight loss results from seawater exposure are:

Sample	R(mpy)	Maximum Localized Attack (mm)
1	6.7	1.02 (Pitting)
2	7.4	1.74 (Pitting)
3	5.4	0.63 (Pitting)
AVG	6.5	1.13

These results show that corrosion rate of 7075 Aluminum in 3.5% sodium chloride solution is very close to the corrosion rate in natural sea water. When the sample was polarized anodically in 3.5% sodium chloride solution, its surface showed a black porous film that failed to adhere to the surface. This tendency is quite obvious in the potentiodynamic plot shown in Figure [14]. Examination of actual sea water-exposed samples shown in Figure [42] also indicates areas of dark oxidation. However, these samples also are characterized by severe localized corrosion and significant pitting (1.13 mm), in agreement with the PDP Plot. The results of scanning electron microscopy are shown in Figures [28] and [29] and indicate clearly the areas of severe localized pitting.

2. 630 BRONZE

The Polarization results for samples of 630 Bronze are shown in Figures [16] and [17]. Photograph of the sea water exposed corroded sample is shown in Figure [43]. Using the PDP and LPM Plots yield the following results:

Method	B _a (V/Decade)	B _c (V/Decade)	I _{corr} (A/cm ²)	R(mpy)
1	0.057	0.321	0.1285	0.062
2	0.057	0.321	4.48	2.120
AVG				1.09

Direct weight loss results from sea water exposures are:

Sample	R(mpy)	Maximum Localized attack (mm)
1	0.5	<0.01 (Pitting)
2	0.4	0.09 (Pitting)
3	0.6	0.02 (Pitting)
AVG		0.04

During the Polarization experiment the 630 Bronze specimen showed a uniformly distributed passive film as indicated by the PDP Plot shown in Figure [16]. The results from Polarization techniques and sea water exposures were in good agreement considering that the polarization techniques were conducted in 3.5% sodium chloride solution.

Although seawater exposed samples exhibit pitting behaviour, these pits were very small. Green corrosion products were found near and around the suspension holes in the specimens. The rest of the specimen was in fairly good condition except for the slight localized attack mentioned above. Microscopic examination are shown in Figures [30] and [31]. All the sea water exposed samples exhibit an area on one end in which the corrosion behavior is different from the rest of the specimen. This area is clearly evident in Figure [43] and retains a distinct difference even after

acid cleaning. No definite explanation can be given for the effect.

3. Fe-Cr-Mo

The laboratory results for the Fe-Cr-Mo high damping alloy are depicted in Figures [18] and [19]. Surface appearance of sea water exposed samples is shown in Figure [44]. The use of PDP and LPM plots yields following results:

Method	Ba (V/Decade)	Bc (V/Decade)	icorr (A/cm ²)	R(mpy)
1	0.234	0.110	.04	.018
2	0.234	0.110	0.613	.276
				AVG 0.147

Direct weight loss results from sea water exposure are:

Sample	R(mpy)	Maximum Attack (mm)
1	3.0	2.32 (Pitting)
2	3.6	3.39 (Pitting)
AVG	3.3	AVG 2.855

The results from the PDP curve show that this alloy has a tendency for film formation but the film breaks down quickly, resulting in severe general pitting on the surface

of the spicemen. Even though this alloy showed nearly identical polarization behaviour as 304 stainless steel, it was highly susceptible to severe pitting.

Sea water exposed samples displayed an unusual behaviour, in that the whole surface was almost unaffected, but at just one or two points there was severe localized corrosion and pitting, these pits being 2 - 3 mm deep. Apparently, same point of instability in the surface oxide film initiates a small pit on the surface of the alloy, which grows rapidly with time due to many factors, such as the adverse area effect, etc. The before-cleaning appearance confirms this attack, indicated by the build up of iron corrosion product on the specimen. In the 65 days sea water exposed samples it was observed that the attack is concentrated at or near the edges, but, at 150 days sea water exposure, the attack was often in the middle of the broad surfaces of the specimen. SEM Photographs shown in Figure [33] support the above results.

4. Fe-Cr-Al

The electrochemical results for the Fe-Cr-Al high damping alloy are shown in Figures [20] and [21]. The surface appearances of the sea water exposed samples are displayed in Figure [45]. The PDP and LPM plots yield the following results:

Method	E _a (V/Decade)	E _c (V/Decade)	i _{corr} (A/cm ²)	R(mpy)
1	0.214	0.1285	0.6598	0.313
2	0.214	0.1285	1.18	0.551

AVG 0.432

Direct weight loss results from sea water exposure are:

Sample	R(mpy)	Maximum Attack (mm)
1	1.0	0.07 (Pitting)
2	2.6	1.01 (Pitting)
3	3.0	1.31 (Pitting)
AVG 2.2		AVG 0.797

This alloy showed features similar to those experienced by the Fe-Cr-Mo samples. The PDP plot for this alloy did not show distinct region of film formation, yet it was susceptible to severe pitting alround the specimen as in the case of the Fe-Cr-Mo alloy.

Sea water exposure Figure [45] characterized by similar visual appearance as that shown by the Fe-Cr-Mo specimen, that is, gross corrosion products outcropping from just one or two spots. Upon cleaning of the specimen these spots were found to be large localized corrosion and pitting

sites. The unusual behavior of the two Fe-Cr based alloys is difficult to explain; it is possible that the presence of an impurity in the alloy or the oxide film results in such behavior.

SEM photographs shown in Figures [34] and [35] showed that the specimen was subjected to guide distinct intergranular attack. Although the pitting was similar to that of the Fe-Cr-Mo alloy, its depth was much less.

5. Cu-Mn-Al (INCRAMUTE)

The Polarization results for the Cu-Mn-Al alloy, also known as INCRAMUTE are shown in Figures [22] and [23]. Visual appearance of sea water exposed samples are depicted in Figure [46]. The PDP and LPM plots yield the following results:

Method	B _a (V/Decade)	B _c (V/Decade)	i _{corr} (A/cm ²)	R(mpy)
1	0.0137	1.379	6.0618	9.08
2	0.0137	1.379	10.8	16.2
				AVG 12.6

Direct weight loss results from sea water exposure are:

Sample	R(mpy)	Maximum Attack (mm)
1	3.7	General Corrosion
2	3.4	with very
3	3.7	slight pitting
AVG		3.6

The PDP plot showed a limited range where a protective film does start to form, but the specimen showed no signs of pitting. During the polarization experiment, the sample is covered with thick black layer and the same tendency is observed with the sea water exposed samples as shown in Figure [46]. It can be seen that approximately 90-100% of the sample is covered with dark brown or black corrosion product layer. SEM photographs show the same results.

6. 304 STAINLESS STEEL

The Polarization results for 304 stainless steel are shown in Figures [24] and [25]. Surface appearance of sea water exposed samples is shown in Figure [47]. The PDP and LPM plots yield the following results:

Method	Ba (V/Decade)	Bc (V/Decade)	icorr (A/cm ²)	R(mpy)
1	0.4117	0.117	0.1	0.05
2	0.4117	0.117	0.02	0.0095

AVG 0.029

Direct weight loss results from sea water exposure are:

Sample	R(mpy)	Maximum Attack (mm)
1	<0.1	0
2	<0.1	0
3	<0.1	0
AVG <0.1		AVG 0

The results from the PDP plot showed that 304 stainless steel has the tendency of film formation and that it is similar to the Fe-Cr-Mo plot. However, the film on the 304 stainless steel is more stable and it has a passive region, over which the sample is protected from pitting.

The observation of sea water exposed samples showed no signs of localized corrosion or pitting. Microscopic examination shown in Figures [38] and [39] were in agreement with the above result.

7. Cu-Mn-Al-Fe-Ni (SONOSTON)

The electrochemical results for samples of the high damping Cu-Mn based alloy (SONOSTON, Cu-Mn-Al-Fe-Ni) are shown in Figures [26] and [27]. The visual appearance of sea water exposed samples is shown in Figure [48]. Using PDP and LPM plots, Methods 1 - 2 yield the following results:

Method	B _a (V/Decade)	B _c (V/Decade)	i _{corr} (A/cm ²)	R(mpy)
1	0.066	0.273	4.64	2.36
2	0.66	0.273	2.11	1.07
				AVG 1.715

Direct weight loss results from sea water exposure are:

Sample	R(mpy)	Maximum Attack (mm)
1	2.5	General Corrosion
2	2.3	General Corrosion
3	2.7	General Corrosion
<hr/>		
AVG	2.5	

There was good agreement between corrosion rates calculated for natural sea water exposures and 3.5% sodium chloride solution. There was no pitting tendency observed in the PDP plot, which is in agreement with the sea water exposure results.

Surface appearance of the sea water exposed samples showed that approximately 90 - 100% of the specimen surface was covered with dark brown or black corrosion. SEM photography shown in Figures [40] and [41] did not show any sign of pitting or localized corrosion.

B. GALVANIC COUPLING

In order to successfully use electrochemical techniques to predict galvanic corrosion, measurements must be made in an environment closely simulating the actual one. These measurements were made in 3.5% sodium chloride solution and hence the results of galvanic corrosion for the coupled alloys are strictly valid for this environment only.

However, these results can prove to be useful to predict galvanic corrosion behavior of the high damping alloys in an environment closely related to this one.

In many cases, simple measurement of the potential of each member in a galvanic couple is sufficient to predict the galvanic corrosion behavior. The resulting galvanic series of metals for a particular environment can be quite useful. However, frequently more precise information, such as the variation of potential/current with time, is required; this is discussed in this section.

Measurement of galvanic currents can furnish more useful information regarding galvanic corrosion. Recent developments with zero resistance ammeters allows continuous measurement of the galvanic current during the short circuiting conditions. This current, however, is not always equivalent to the corrosion current because it is the algebraic sum of the currents due to anodic and cathodic reactions. Thus, where cathodic currents are significant, the measured galvanic current may be appreciably smaller than the true corrosion current.

1. Select Galvanic Couples

In the present case, all the high damping alloys under examination were first coupled to 304 stainless steel independently and then to 7075 Aluminum. The curves for each couple are shown in Figures [49] to [59]. The curves for current Vs time for each group was then summarized in

figures [60] and [61]. The magnitude of the galvanic current provides an indication of the severity of galvanic corrosion which occurs in the specific 3.5% sodium chloride environment. The results for each couple is discussed seperately.

In Figure [49], the zero resistance current and the mixed potential are plotted Vs time for 630 Bronze and 7075 Aluminum in 3.5% sodium chloride environment. The data show that 7075 Aluminum is anodic to 630 Bronze in this environment. The rise in galvanic current after about eight hours signifies the initiation of localized corrosion of the aluminum alloy in this environment. Both the mixed potential and galvanic current stabilizes after about 10 hours. The galvanic current at the end of 14 hours is about 107 A.

In Figure [50], the data is plotted for Inframute and 7075 Aluminum. Although the mixed potential remains quite stable with time, the galvanic current changes over the time period shown. Initially, the aluminum alloy is anodic to Inframute. However, after about an hour, the galvanic current indicates that a reversal takes place so that the Inframute is then anodic to the aluminum alloy in this environment. This situation appears to continue throughout during the interval of immersion. This phenomenon is not unexpected, since the metals are so close to each other in the galvanic series for this particular

environment. Hence, it is possible that formation of film on the initial anode changes the potential, and the reversal takes place. During the 14 hours of immersion the galvanic current varies in the range of 20 A.

The data for Sonoston and 7075 Aluminum is shown in Figure [51]. Although the mixed potential remains quite stable with time, the galvanic current reduces after about 8 hours. This is followed immediately by a sharp rise and fall of the galvanic current signifying the start of corrosion of the 7075 Aluminum. The current, however, reduces to stable value of 55 A at the end of 14 hours of immersion.

The data for Fe-Cr-Mo and 7075 Aluminum is displayed in Figure [52]. The data shows that the aluminum alloy is anodic to the Fe-Cr-Mo alloy. The potential drops continuously and becomes stable after 10 hours. However, galvanic current reduces to a lower level after 5 hours, followed by a sharp rise. This indicates the initiation of localized corrosion of the aluminum alloy sample. This is repeated at the end of 12 hours. The galvanic current at the end of 14 hours of immersion is about 40 A.

In Figure [53], the galvanic current and potential are plotted Vs time for 304 stainless steel and 7075 Aluminum. The data show that Aluminum is anodic to steel. The potential becomes stable after about 10 hours. The galvanic current reduces at the time of immersion but jumps

suddenly after about half an hour, indicating the initiation of localized corrosion. At the end of 14 hours the current is still changing and is of the order of 42 A.

The data for Fe-Cr-Al and 7075 Aluminum is recorded in Figure [54]. In this couple, the aluminum alloy is anodic to the Fe-Cr-Al. Both the mixed potential and galvanic current for this couple becomes stable after several hours and current is of the order of 45 A.

The remainder of the discussion in this section pertains to the discussion, each in time, of the galvanic couples formed by coupling 304 stainless steel with the various other alloys.

In Figure [55], the data is plotted for Sonoston and 304 stainless steel. Sonoston is anodic to steel in this environment. Both the potential and galvanic current become stable after about 5 hours. There is uniform current of about 40 A at the end of 14 hours of immersion.

In Figure [56], the data shown is for 630 Bronze and 304 stainless steel. In this environment the bronze alloy is anodic to the stainless steel, but with a very low level of galvanic current, due to the close relative position in the Galvanic series. There is not much corrosion behavior observed during the 14 hours of immersion. Both the potential and galvanic current become stable after several hours.

The data for 304 stainless steel and Inconel is shown in Figure [57]. In this environment Inconel is anodic to the stainless steel. The galvanic current rises suddenly at the end of five hours of immersion, signifying the initiation of localized corrosion. At this point the formation of a black film on the anodic member is observed. The galvanic current and potential seems to stabilize after about 12 hours. At the end of 14 hours of immersion the galvanic current is about 37 A.

The data for 304 stainless steel and the Fe-Cr-Al alloy is demonstrated in Figure [58]. Initially the Fe-Cr-Al is anodic with respect to the stainless steel but, after about 0.5 hours, the galvanic current indicates that a reversal takes place, so that the stainless steel becomes anodic to the Fe-Cr-Al in this environment. The galvanic current reduces to a negligible value thereafter. However, the potential is decreasing continuously even after 14 hours of immersion.

In Figure [59], the data is plotted for 304 stainless steel and Fe-Cr-Mo. The data shows that the Fe-Cr-Mo is anodic with respect to the stainless steel in this environment. Both the galvanic current and potential become stable after a couple of hours of immersion. There is a very small galvanic current that flows at the end of 14 hours of immersion.

Figures [49] and [50] show that time dependent factors such as initiation of localized corrosion and anode-cathode reversal must not be overlooked and that long term tests are frequently required. This is especially true when localized corrosion such as pitting is possible in the galvanic couple. Frequently, several weeks induction period is observed before galvanic pitting is initiated.

2. Galvanic Series of Selected High Damping and Baseline Alloys in Quiescent 3.5% Sodium Chloride Solution

Temperature about 21.5 ± 0.5 C

<u>Alloy</u>	<u>Steady State Electrode Potential Vs Saturated Calomel Electrode (V)</u>
7075 Aluminum	- 0.780
Cu-Mn-Al (INCRAMUTE)	- 0.779
Cu-Mn-Al-Fe-Ni (SONOSTON)	- 0.673
Fe-Cr-Al (VACROSIL 2)	- 0.371
Fe-Cr-Mo (VACROSIL1)	- 0.276
630 Series Bronze	- 0.245
340 Stainless Steel (active)	- 0.241
304 Stainless Steel (Passive)	- 0.053

V. CONCLUSIONS AND RECOMMENDATIONS

The following conclusions have been drawn from the data presented in the previous chapters:

1. Fe-Cr-Mo and Fe-Cr-Al experienced severe localized corrosion and pitting. Fe-Cr-Al show intergranular attack.
2. Cu-Mn-Al based alloys and 630 series Bronze experienced low to moderate corrosion rate..
3. When coupled with 7075 Aluminum, all couples show a higher galvanic current initially but reduces with time to steady value, except for Inconel which reverses polarity from time to time.
4. When coupled with 304 stainless steel the three alloys Fe-Cr-Mo, Fe-Cr-Al, 630 Bronze showed negligible or very low galvanic current where as 7075 Aluminum, Inconel and Inconel showed moderate galvanic current.

Suggested topic for future research are:

1. 30, 60 and 120 days of immersion period be observed so that pitting behaviour can be observed in the galvanic corrosion technique.
2. Development of a computer assisted method for determining the Tafel constants.

APPENDIX A

FIGURES

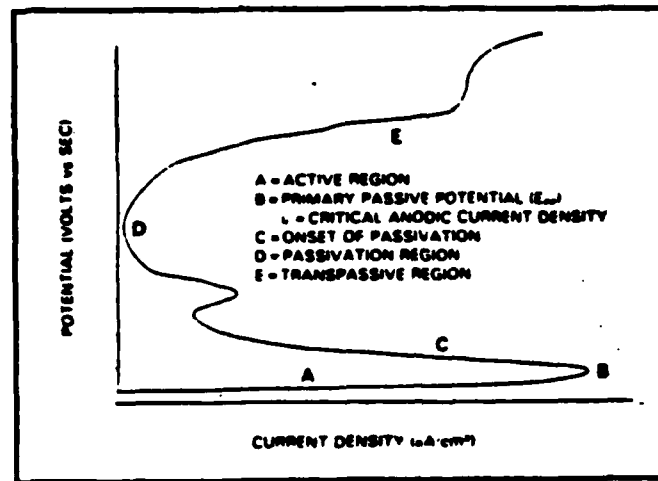


Figure 1. Potentiodynamic Polarization Plot

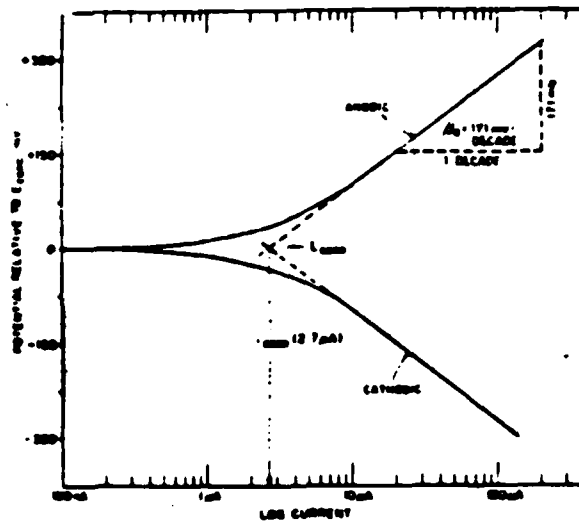


Figure 2. PDP Plot Showing Tafel Regions

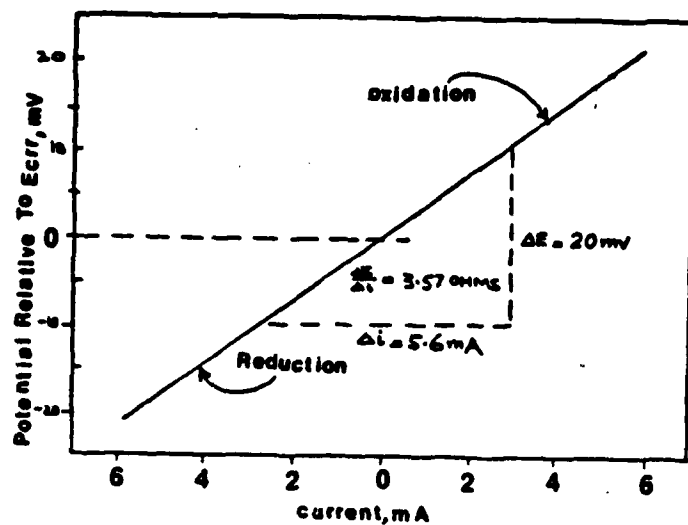


Figure 3. Polarization Resistance Plot

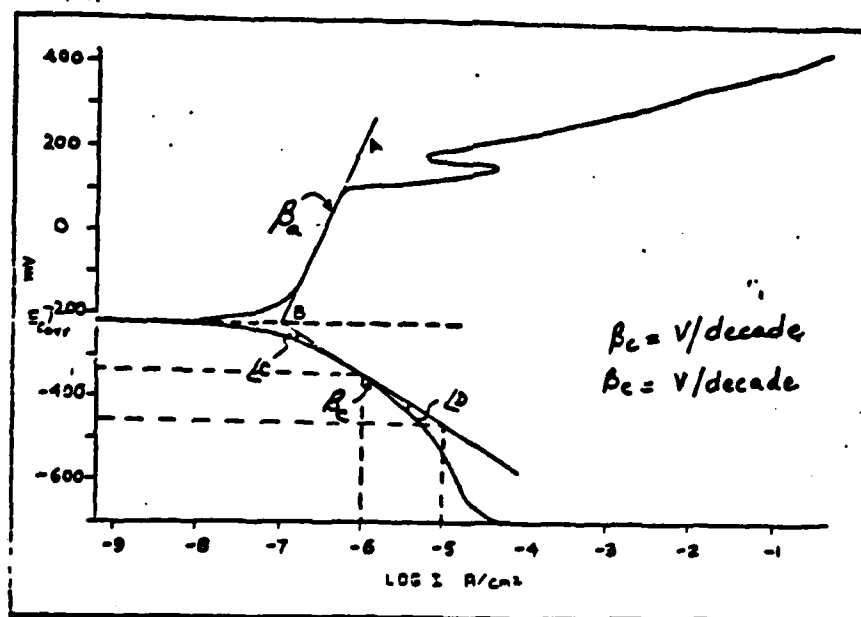


Figure 4. Method for Determining Tafel Constants

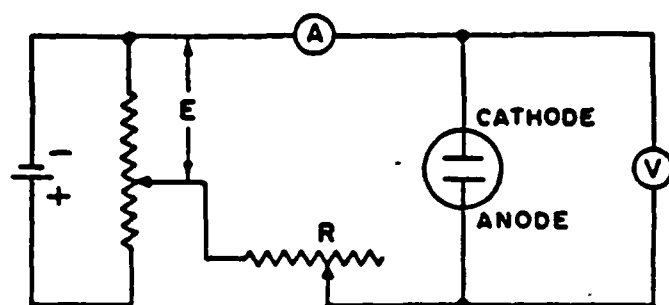


Figure 5. Basic Zero Resistance Ammeter Circuit

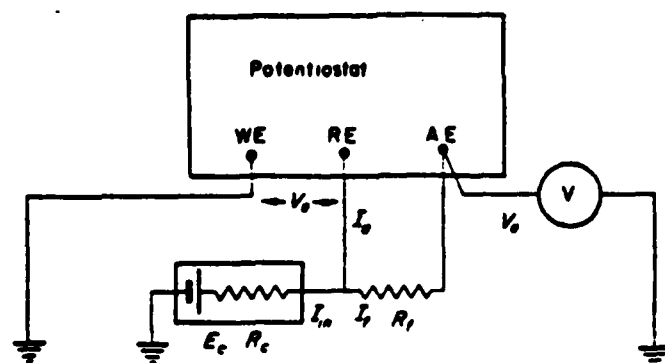


Figure 6. Circuit of a Potentiostat as a Zero Resistance Ammeter

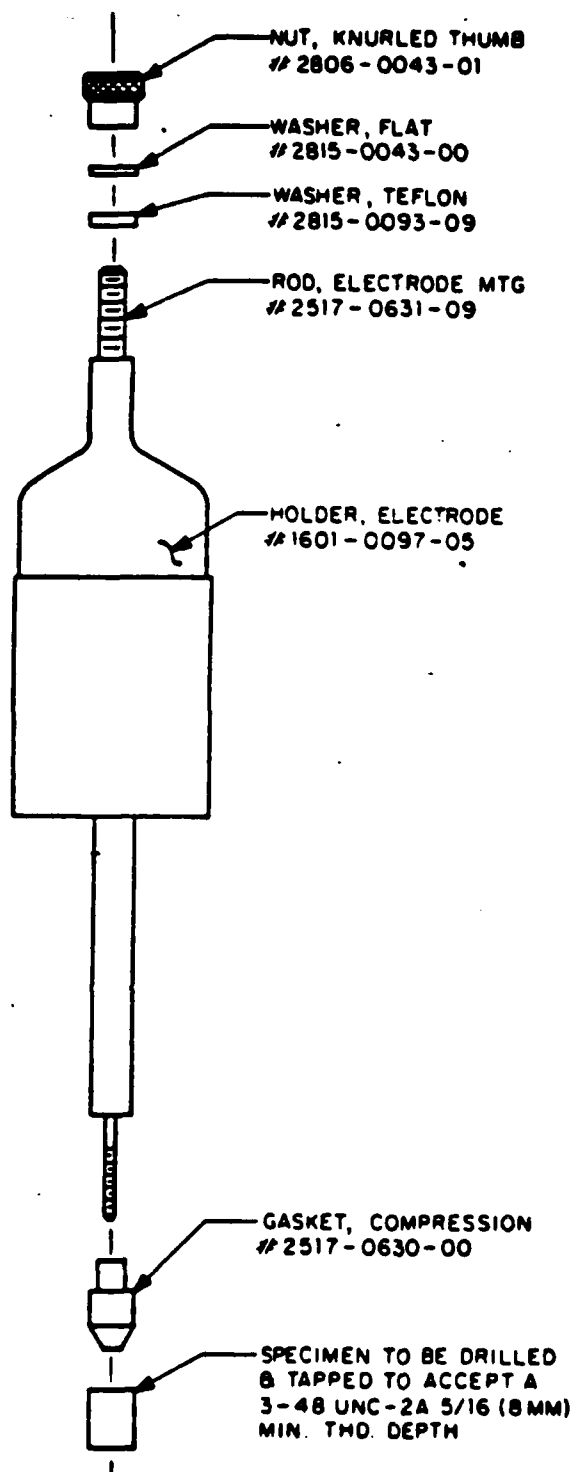


Figure 7. Working Electrode Sample Holder

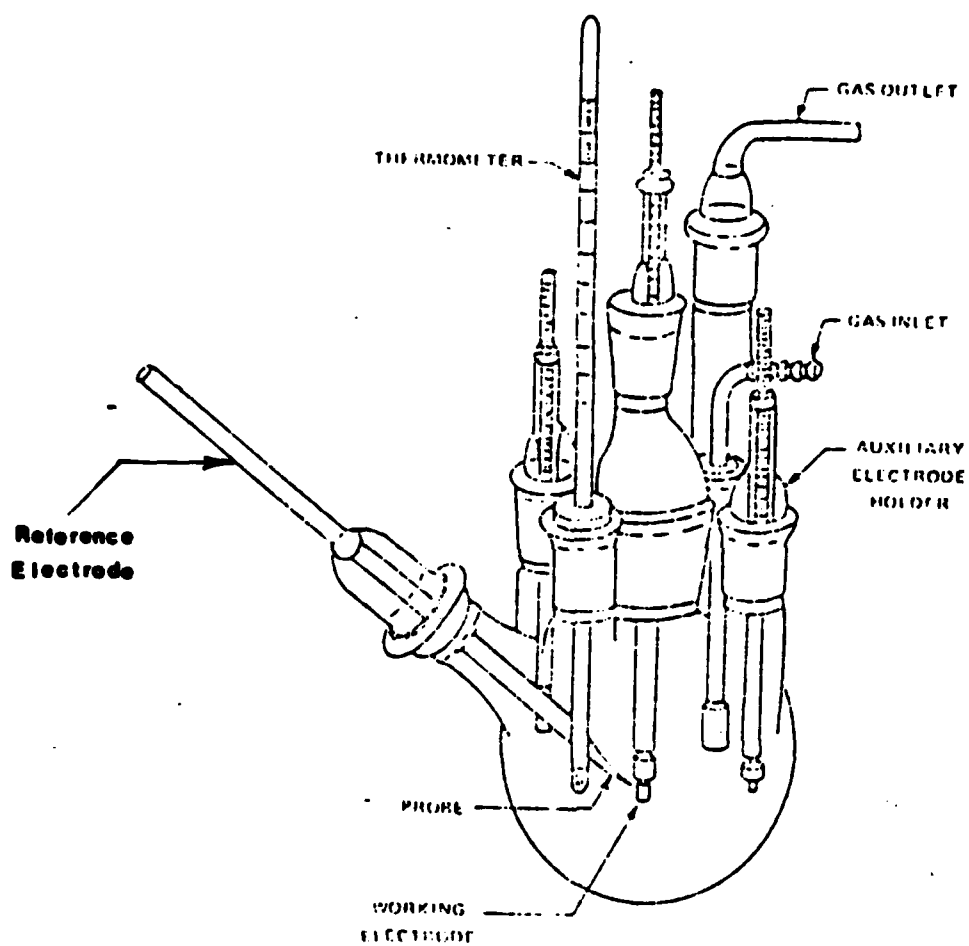


Figure 8. Standard K47 Corrosion Cell

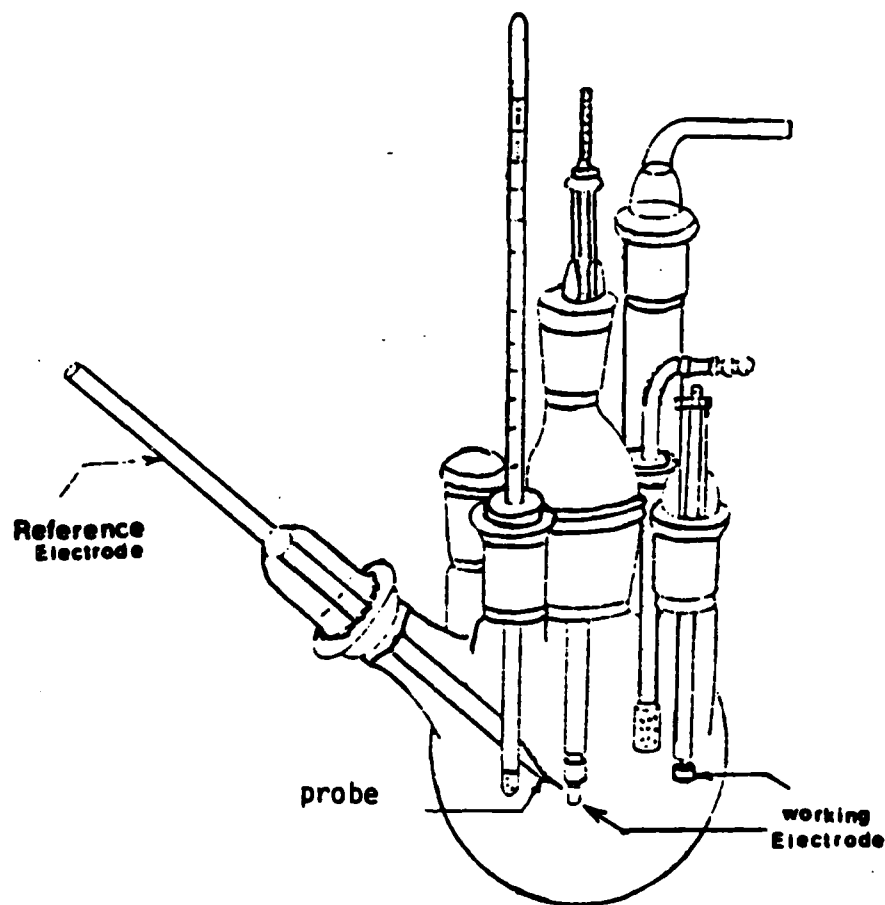


Figure 9. Galvanic Corrosion Cell Arrangement

POTENTIODYNAMIC		SAMPLE ID: UNNAMED	
CREATE EDIT: PAGE 1		CONTENT: EG&G PARC MODEL 351	
SELECTED TECHNIQUE			
POTENTIODYNAMIC			
<input type="text"/>	INITIAL E	<input type="text"/>	INITIAL DELAY
	-250 mV/EC		3600 SEC
<input type="text"/>	SCAN RATE		
	0.166 mV/SEC		
<input type="text"/>	FINAL E		
	1.2 V		
<input type="text"/>	SMOOTH	<input type="text"/>	IR COMPENSATION
	7 POINTS		DISABLED
<input type="button" value="MAIN MENU"/>		<input type="button" value="NEXT PAGE"/>	
		<input type="button" value="SELECT NEW TECHNIQUE"/>	

Figure 10. Format for a PDP Experiment

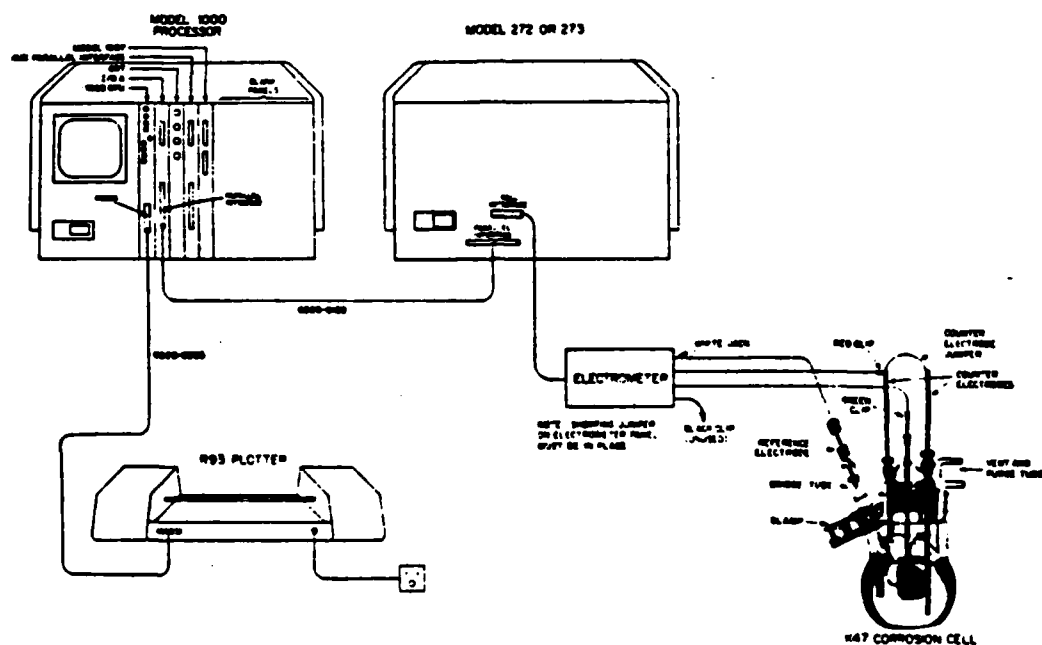


Figure 11. Basic System Installation for PDP

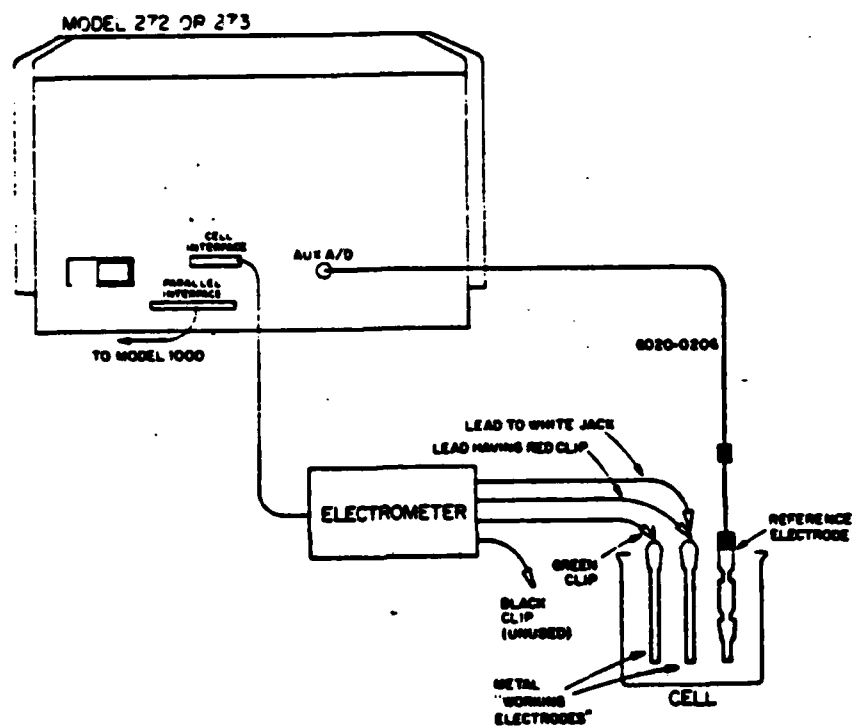


Figure 12. Galvanic Corrosion Set Up

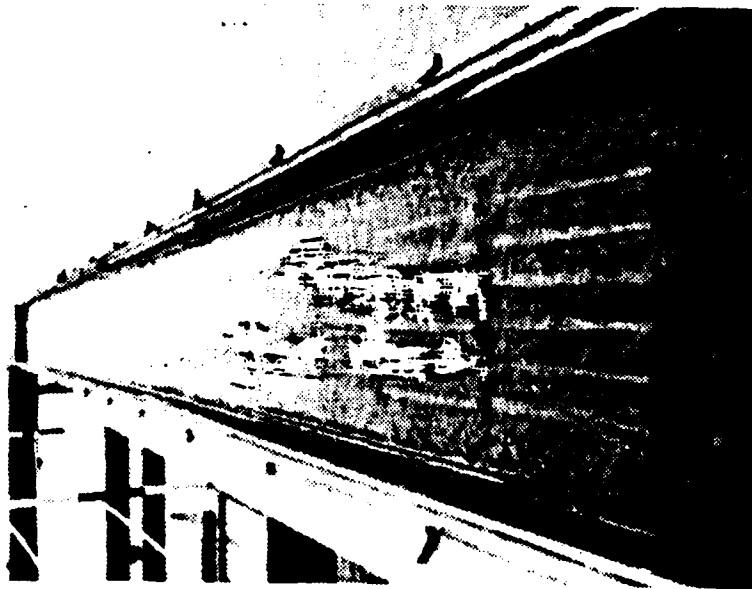
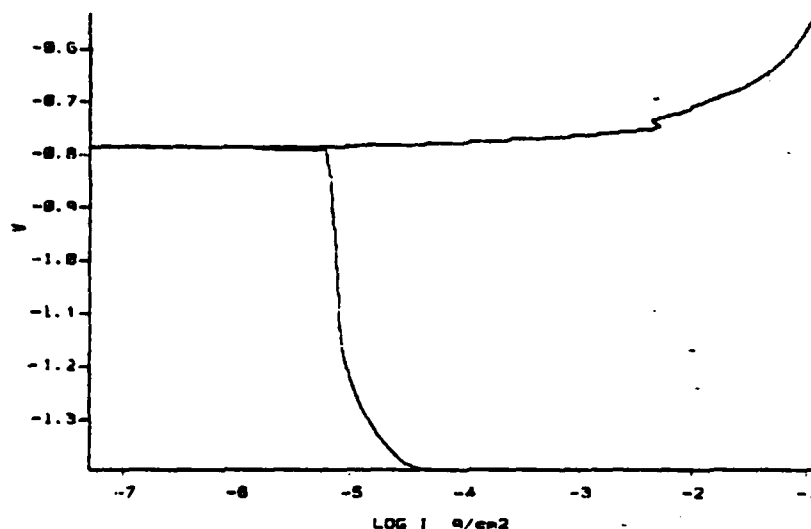


Figure 13. Low Velocity Sea Water Trough

MODEL 351 CORROSION MEASUREMENT SYSTEM	AL7075 12 SEP 1987
COMMENT: 3.5 NAACL SOLN	



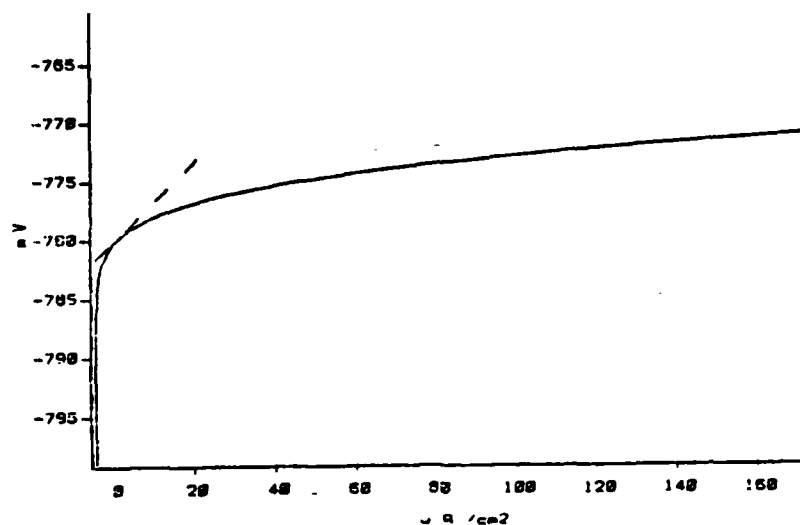
POTENTIODYNAMIC					
DATE CREATED	12	AUG	1987	RUN DATE	12 AUG 1987
IR COMP	= DISABLED				
FINAL E	= 750 mV ~ Ec				
INITIAL E	= -600 mV ~ Ec				
INITIAL DELAY	= 3600 SEC				
SCAN RATE	= 0.5 mV/SEC				
EQUIV WEIGHT	= 8.994 g/EQUIV				
DENSITY	= 2.89 g/cm3				
AREA	= 8.6 cm2				
				Ecorr	= -0.792 V
				E(1=0)	= 0 V
				CORR RATE	= 0 MPY

Figure 14. PDP Plot for 7075 Aluminum

MODEL 351
CORROSION MEASUREMENT SYSTEM

AL7075LP
12 SEP 1987

COMMENT:
3.5 NAACL SOLN

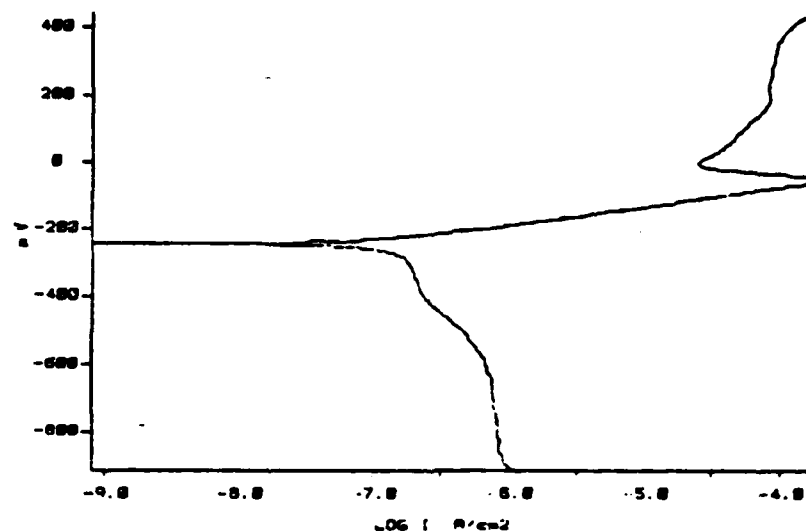


POLARIZATION RESISTANCE

DATE CREATED 30 AUG 1987			RUN DATE 30 AUG 1987		
IR COMP	=	DISABLED	Ecorr	=	-0.78 V
SIGNAL E	=	20 mV ~ Ec	EII=20	=	-0.78 V
INITIAL E	=	-20 mV ~ Ec			
INITIAL DELAY	=	3600 SEC			
SCAN RATE	=	0.1 mV/SEC	CORR RATE	=	0 MPY
			AP calc.	=	332 E0 Ohms
EQUIV WEIGHT	=	8.994 g/EQUIV	ANODIC-BETA	=	0.009 V/DEC
DENSITY	=	2.45 g/cm3	CATHODIC-BETA	=	2.36 V/DEC
AREA	=	9.388 cm2	Icorr calc.	=	11.7 E-6 A /cm2
			CORR RATE calc	=	5.68 E0 MPY
POINTS	AMPS	VOLTS			
2	-5 E-6	-799 E-3			
58	172 E-6	-771 E-3			

Figure 15. Polarization Resistance Plot for
7075 Aluminum

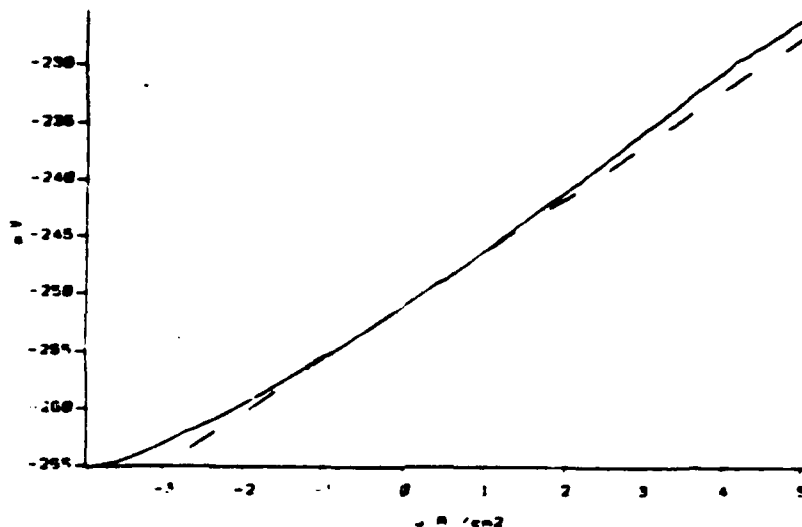
MODEL 351 CORROSION MEASUREMENT SYSTEM	BRZ630PD 12 SEP 1987
COMMENT: 3.5 NAACL SOLN VENTED	



POTENTIOSTATIC			
DATE CREATED	21 JUL 1987	RUN DATE	21 JUL 1987
IR COMP	= DISABLED		
FINAL E	= 700 mV ~ Ec	Ecorr	= -0.261 V
INITIAL E	= -650 mV ~ Ec	E(1=0)	= 0 V
INITIAL DELAY	= 2400 SEC		
SCAN RATE	= 0.75 mV/SEC	CORR RATE	= 3 MPY
EQUIV WEIGHT	= 27.67 g/EQUIV		
DENSITY	= 5.46 g/cm³		
AREA	= 619.7 cm²		

Figure 16. PDP Plot for 630 Bronze

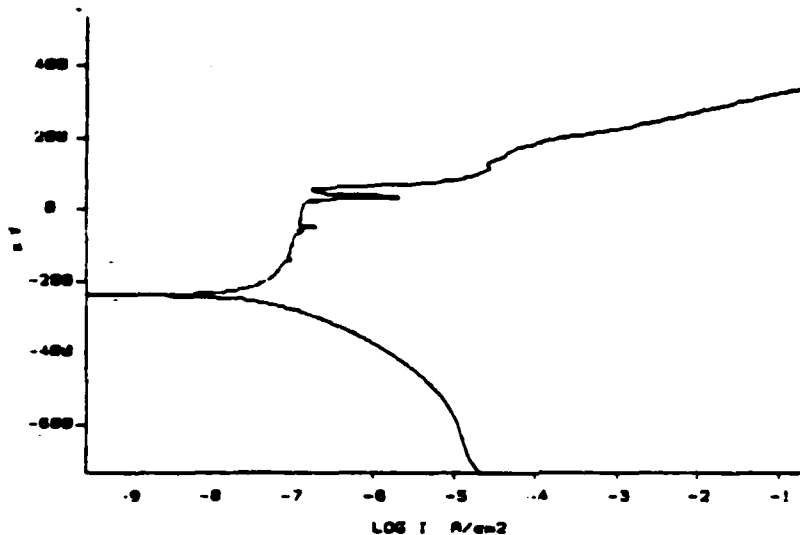
MODEL 351 CORROSION MEASUREMENT SYSTEM	BRNZ630P 12 SEP 1987
COMMENT: 3.5 NACL SOLN	



POLARIZATION RESISTANCE					
FILE CREATED	1	AUG	1987	RUN DATE	1
IR COMP	DISABLED				
FINAL E	20 mV - Ec				
INITIAL E	-20 mV - Ec				
INITIAL DELAY	3600 SEC				
SCAN RATE	0.1 mV/SEC				
EQUIV WEIGHT	27.67 g/EQUIV				
DENSITY	7.59 g/cm³				
AREA	4.027 cm²				
				Ecorr	-0.245 V
				E(1-0)	-0.251 V
				CORR RATE	0.000000
				Rp calc.	4.78 E3 Ohms
				ANODIC BETA	0.057 V/DEC
				CATHODIC BETA	0.321 V/DEC
				Icorr calc.	4.48 E-6 A/cm²
				CORR RATE calc	2.12 E0 mm/y
ROOT	AMPS	VOLTS			
0	-4 E-6	-265 E-3			
79	5 E-6	-226 E-3			

Figure 17. Polarization Resistance Plot 630 Bronze

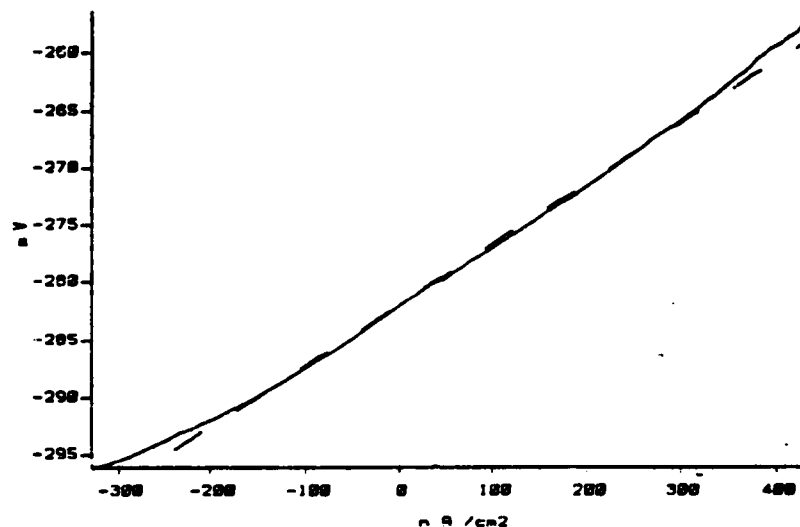
MODEL 351 CORROSION MEASUREMENT SYSTEM	VCMOPD 12 SEP 1987
COMMENT 3.5 NAACL SOLN	



POTENTIODYNAMIC			
DATE CREATED	30 JUL 1987	RUN DATE	30 JUL 1987
IR COMP	DISABLED		
FINAL E	700 mV ~ Ec	Ecorr	-0.16 V
INITIAL E	-600 mV ~ Ec	E(1-0)	0 V
INITIAL DELAY	3600 SEC		
SCAN RATE	0.5 mV/SEC	CORR RATE	0 MPY
EQUIV WEIGHT	26.34 g/EQUIV		
DENSITY	5.84 g/cm³		
AREA	5.814 cm²		

Figure 18. PDP Plot for Fe-Cr-Mo

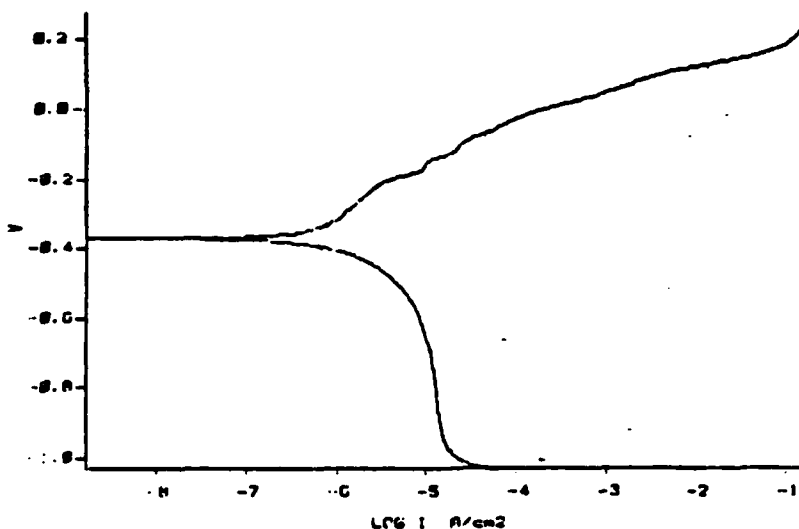
MODEL 351 CORROSION MEASUREMENT SYSTEM	VAC1LP 12 SEP 1987
COMMENT: 3.5 NAACL SOLN	



POLARIZATION RESISTANCE			
DATE CREATED	29	AUG	1987
IR COMP	= DISABLED		
FINAL E	= 20 mV ~ E _c		
INITIAL E	= -20 mV ~ E _c		
INITIAL DELAY	= 3500 SEC		
SCAN RATE	= 0.1 mV/SEC		
SQUIV WEIGHT	= 25.34 g/EQUIV		
DENSITY	= 7.6 g/cm ³		
AREA	= 4.36 cm ²		
		RUN DATE	29 AUG 1987
		E _{corr}	= -0.276 V
		E(I=0)	= -0.282 V
		CORR RATE	= 0 MPY
		RP calc.	= 53.1 E3 Ohms
		ANODIC-BETA	= 0.234 V/DEC
		CATHODIC-BETA	= 0.11 V/DEC
		i _{corr} calc.	= 613 E-9 A/cm ²
		CORR RATE calc	= 276 E-3 MPY
00PT#	AMPS	VOLTS	
0	-328 E-9	-296 E-3	
79	438 E-9	-257 E-3	

Figure 19. Polarization Resistance Plot for Fe-Cr-Mo

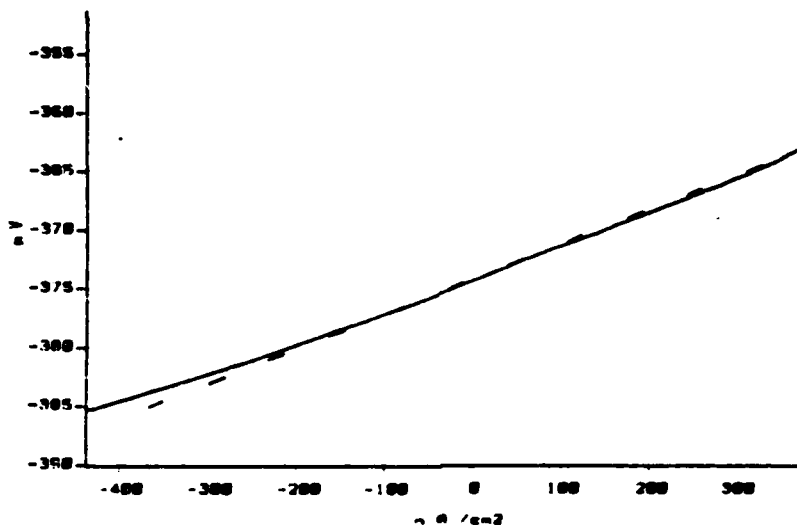
MODEL 351 CORROSION MEASUREMENT SYSTEM	VACAL2 12 SEP 1987
COMMENT: 3.5 NAACL SOLN	



POTENTIODYNAMIC			
DATE CREATED	12 AUG 1987	RUN DATE	12 AUG 1987
IR COMP	= DISABLED		
FINAL E	= 700 mV - Ec	Ecorr	= -0.428 V
INITIAL E	= -600 mV - Ec	E(1=0)	= 8 V
INITIAL DELAY	= 3600 SEC		
SCAN RATE	= 0.5 mV/SEC	CORR RATE	= 8 MPY
EQUIV WEIGHT	= 26.15 g/EQUIV		
DENSITY	= 5.37 g/cm3		
AREA	= 4.997 cm2		

Figure 20. PDP Plot for Fe-Cr-Al

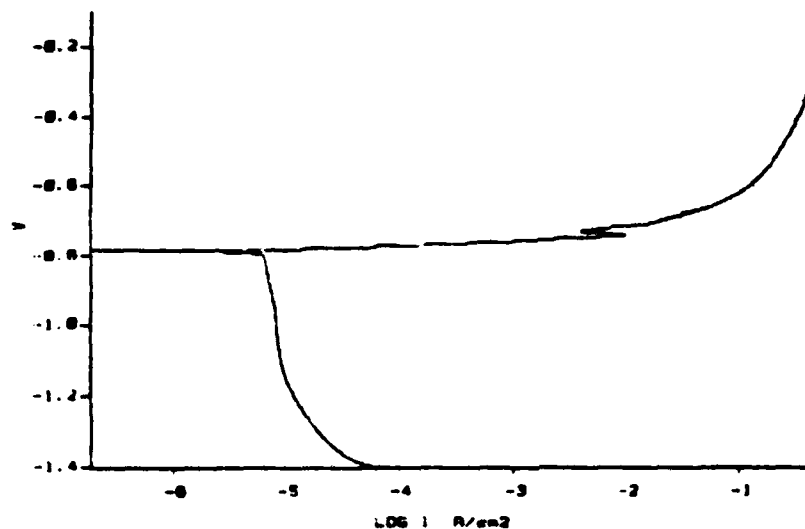
MODEL 351 CORROSION MEASUREMENT SYSTEM	VACALLP 12 SEP 1987
COMMENT: 3.5 NAACL SOLN	



POLARIZATION RESISTANCE			
DATE CREATED	30 AUG 1987	RUN DATE	30 AUG 1987
IR COMP	= DISABLED		
FINAL E	= 28 mV - Ec	Ecorr	= -0.37 V
INITIAL E	= -28 mV - Ec	E11-01	= -0.574 V
INITIAL DELAY	= 3600 SEC		
SCAN RATE	= 0.1 mV/SEC	CORR RATE	= 2 uPY
EQUIV WEIGHT	= 26.15 g/EQUIV	Rp calc.	= 29.0 E3 Ohms
DENSITY	= 7.29 g/cm3	ANODIC-BETA	= 3.214 V/DEC
AREA	= 4.853 cm2	CATHODIC-BETA	= 0.128 V/DEC
		icorr calc.	= 1.18 E-6 A/cm2
		CORR RATE calc	= 551 E-3 uPY
REPORT	WPS	VOLTS	
10	-429 E-9	-385 E-3	
54	369 E-9	-363 E-3	

Figure 21. Polarization Resistance Plot for Fe-Cr-Al

MODEL 351 CORROSION MEASUREMENT SYSTEM	INCRMTE 12 SEP 1987
COMMENT: 3.5 NAACL SOLN	



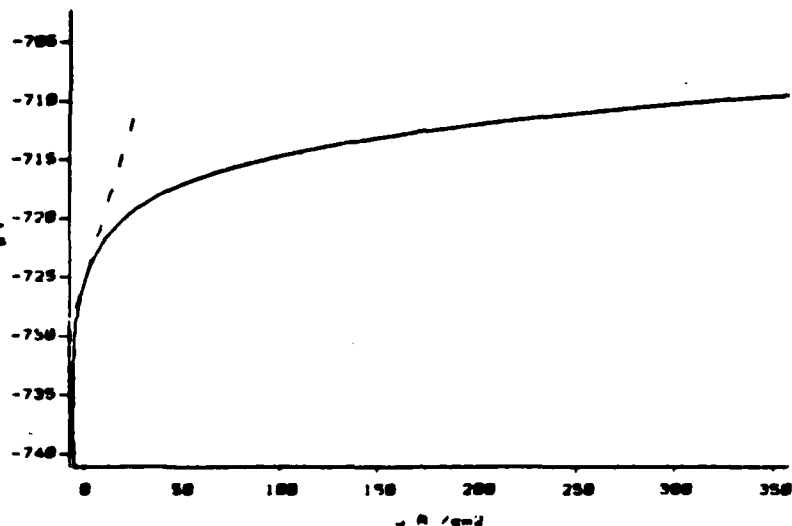
POTENTIODYNAMIC			
DATE TESTED	13 AUG 1987	RUN DATE	15 AUG 1987
TX COMP	• DISABLED		
FINAL E	• 700 mV - E _c	E _{corr}	• -0.002 V
INITIAL E	• -600 mV - E _c	E ₁₁₌₀₁	• 0 V
INITIAL DELAY	• 3000 SEC	CORR RATE	• 0 MPY
SCAN RATE	• 0.5 mV/SEC		
EQUIV WEIGHT	• 29.59 g/EQW		
DENSITY	• 2.59 g/cm³		
AREA	• 3.02 cm²		

Figure 22. PDP Plot for Cu-Mn-Al

MODEL 351
CORROSION MEASUREMENT SYSTEM

INCRMTPR
12 SEP 1987

COMMENT:
3.5 NA CL SOLN



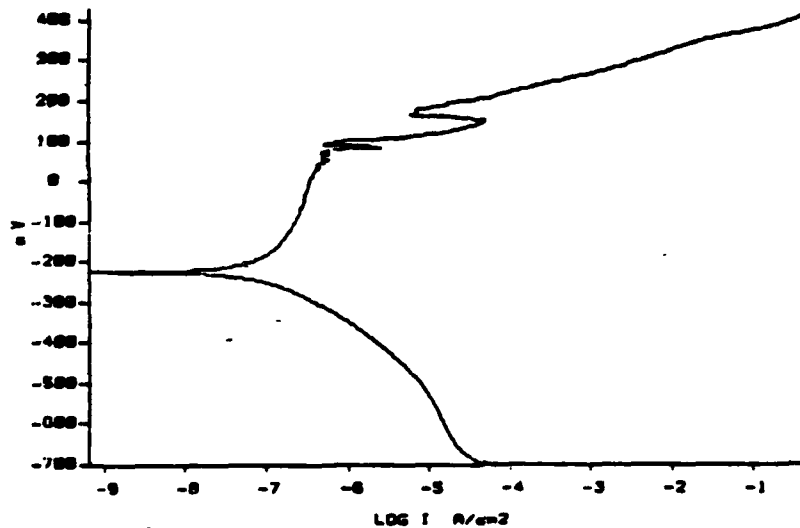
POLARIZATION RESISTANCE					
DATE CREATED	30	AUG	1987	RUN DATE	30 AUG 1987
IN COMP	DISABLED				
INITIAL E	-20 mV - E _c				
INITIAL E	-20 mV - E _c				
INITIAL DELAY	3000 SEC				
SCAN RATE	0.1 mV/SEC				
EQUIV WEIGHT	29.59 g/EQUIV				
DENSITY	2.50 g/cm³				
AREA	2.514 cm²				
				E _{corr}	-0.721 V
				E ₁₁₋₀₁	-0.725 V
				CORR RATE	0 MPY
				R _p calc.	544 E8 Ohms
				ANODIC-BETA	0.014 V/DEC
				CATHODIC-BETA	1.379 V/DEC
				i _{corr} calc.	10.0 E-6 A/cm²
				CORR RATE calc	16.2 E8 MPY
APPLY	APPS	VOLTS			
0	-5 E-6	-741 E-3			
03	344 E-6	-710 E-3			

Figure 23. Polarization Resistance Plot for
Cu-Mn-Al

MODEL 351
CORROSION MEASUREMENT SYSTEM

SST304
12 SEP 1987

COMMENT:
3.5 NAEL SOLN

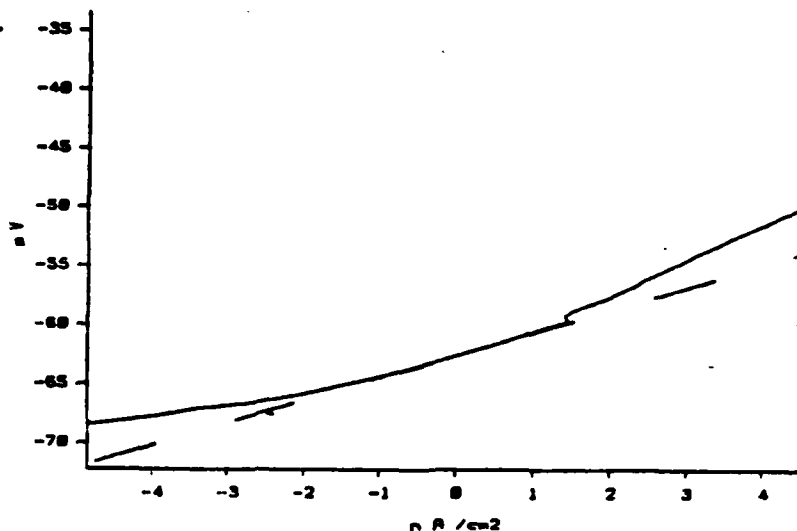


POTENTIODYNAMIC

DATE CREATED	12 AUG 1987	RUN DATE	12 AUG 1987
IR COMP	= DISABLED		
FINAL E	= 750 mV ~ Ec	Ecorr	= -0.1 V
INITIAL E	= -600 mV ~ Ec	E(I=0)	= 0 V
INITIAL DELAY	= 3600 SEC		
SCAN RATE	= 0.5 mV/SEC	CORR RATE	= 0 MPY
EQUIV WEIGHT	= 27.93 g/EQUIV		
DENSITY	= 10.5 g/cm3		
AREA	= 2.632 cm2		

Figure 24. PDP Plot for 304 Stainless Steel

MODEL 351	ST304LPR
CORROSION MEASUREMENT SYSTEM	12 SEP 1987
COMMENT: 3.5 NAEL SOLN	



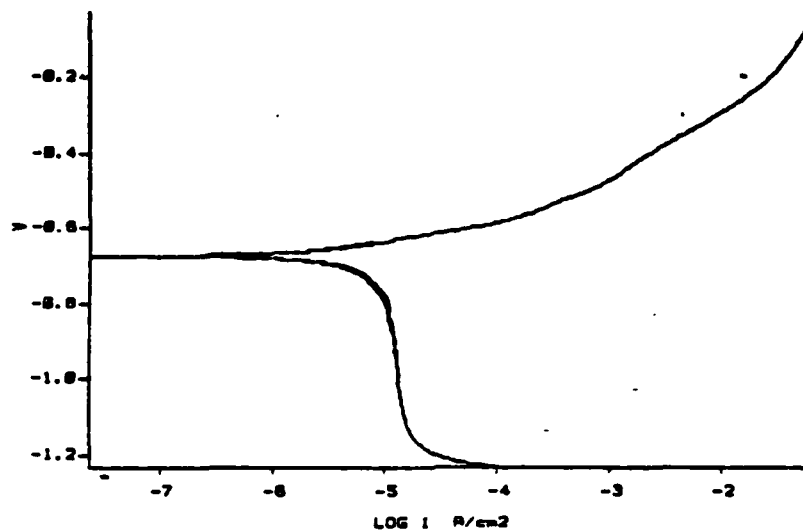
POLARIZATION RESISTANCE			
DATE CREATED	1	SEP 1987	RUN DATE 1 SEP 1987
IR COMP	= DISABLED		
FINAL E	= 20 mV ~ Ec		
INITIAL E	= -20 mV ~ Ec		
INITIAL DELAY	= 3600 SEC		
SCAN RATE	= 0.1 mV/SEC		
EQUIV WEIGHT	= 27.93 g/EQUIV		
DENSITY	= 7.9 g/cm³		
AREA	= 3.102 cm²		
			Ecorr = -0.053 V
			E(I=0) = -0.062 V
			CORR RATE = 0 MPY
			RP calc. = 1.91 E6 Ohms
			ANODIC-BETA = 0.412 V/DEC
			CATHODIC-BETA = 0.117 V/DEC
			Icorr calc. = 20.7 E-9 A/cm²
			CORR RATE calc = 9.51 E-3 MPY
RPT#	AMPS	VOLTS	
0	-10 E-9	-73 E-3	
79	10 E-9	-34 E-3	

Figure 25. Polarization Resistance Plot for 304 Stainless Steel

MODEL 351
CORROSION MEASUREMENT SYSTEM

SONOSTON
12 SEP 1987

COMMENT:
3.5 NACL SOLN



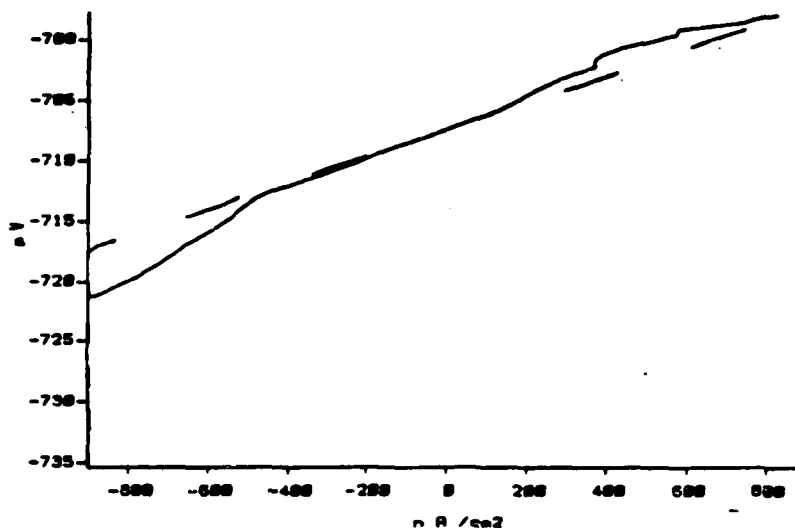
POTENTIODYNAMIC			
DATE CREATED	10 JUL 1987	RUN DATE	10 JUL 1987
IR COMP	= DISABLED		
FINAL E	= 800 mV ~ E _c	E _{corr}	= -0.832 V
INITIAL E	= -400 mV ~ E _c	E(I=0)	= 0 V
INITIAL DELAY	= 3600 SEC		
SCAN RATE	= 0.5 mV/SEC	CORR RATE	= 0 MPY
EQUIV WEIGHT	= 28.32 g/EQUIV		
DENSITY	= 7.27 g/cm ³		
AREA	= 4.28 cm ²		

Figure 26. PDP Plot for Cu-Mn-Al-Fe-Ni

MODEL 351
CORROSION MEASUREMENT SYSTEM

SONOLPR
12 SEP 1987

COMMENT:
3.5 NACL SOLN



POLARIZATION RESISTANCE

DATE CREATED 30 AUG 1987			RUN DATE 30 AUG 1987		
IR COMP	=	DISABLED	Ecorr	=	-0.717 V
FINAL E	=	-20 mV - Ec	EII-01	=	-0.707 V
INITIAL E	=	-20 mV - Ec			
INITIAL DELAY	=	3600 SEC			
SCAN RATE	=	0.1 mV/SEC			
			CORR RATE	=	2 MPY
EQUIV WEIGHT	=	28.32 g/EQUIV	RP calc.	=	11.1 E3 Ohms
DENSITY	=	7.27 g/cm3	ANODIC-BETA	=	0.067 V/DEC
AREA	=	4.20 cm2	CATHODIC-BETA	=	0.273 V/DEC
			Icorr calc.	=	2.11 E-6 A/cm2
			CORR RATE calc	=	1.07 E0 MPY
RPPT#	AMPS	VOLTS			
0	-1 E-6	-737 E-3			
79	1 E-6	-690 E-3			

Figure 27. Polarization Resistance Plot for
Cu-Mn-Al-Fe-Ni

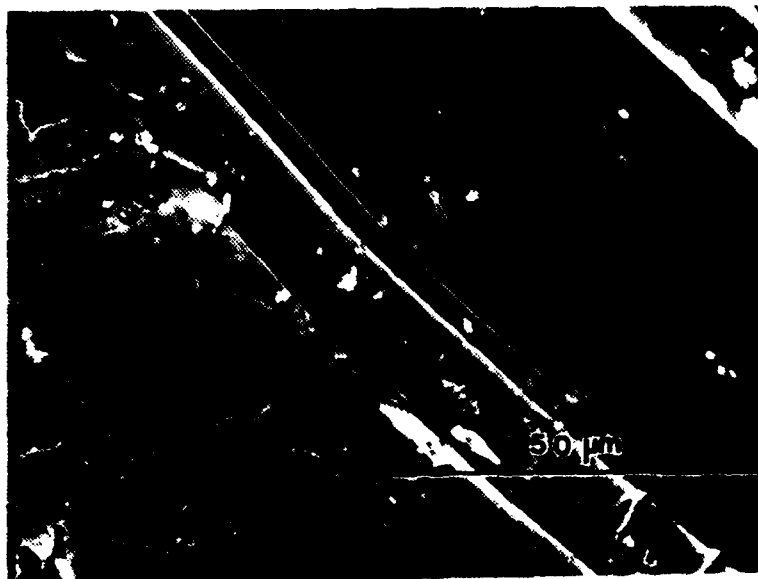


Figure 28. As-Machined Surface of 7075 Aluminum



Figure 29. Corroded Surface of 7075 Aluminum

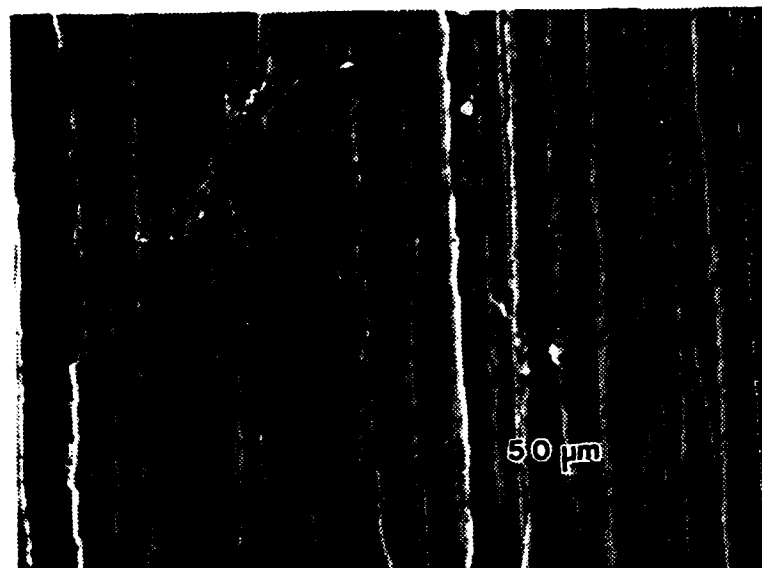


Figure 30. As-Machined Surface of 630 Bronze

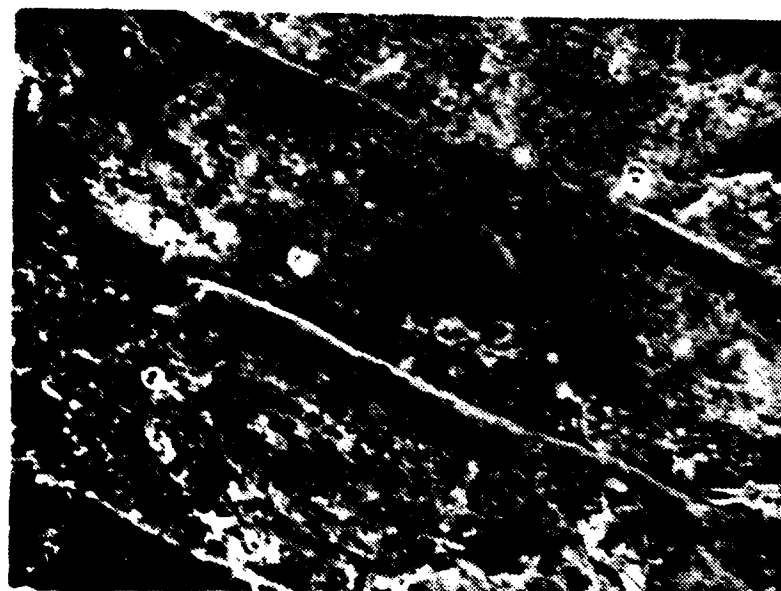


Figure 31. Corroded Surface of 630 Bronze

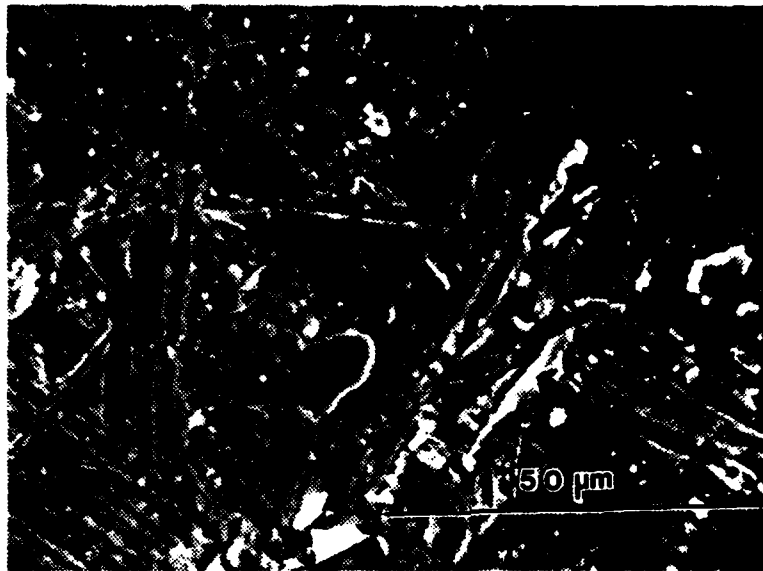


Figure 32. As-Machined Surface of Fe-Cr-Mo

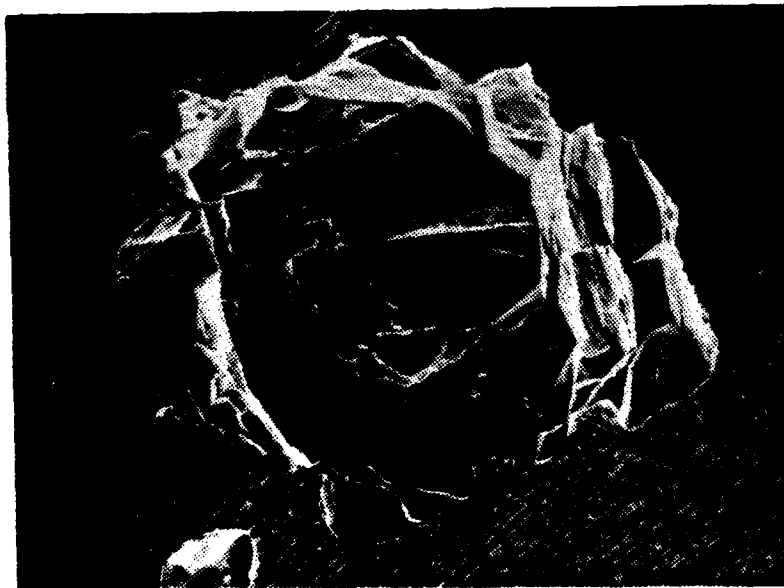


Figure 33. Corroded Surface of Fe-Cr-Mo

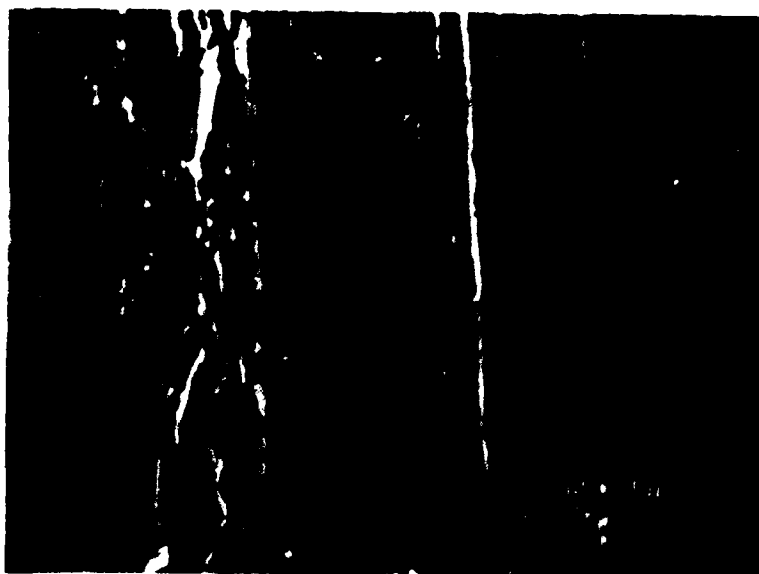


Figure 34. As Machined Surface of Fe-Cr-Al



Figure 35. Corroded Surface of Fe-Cr-Al



Figure 36. As Machined Surface of Cu-Mn-Al



Figure 37 Corroded Surface of Cu-Mn-Al

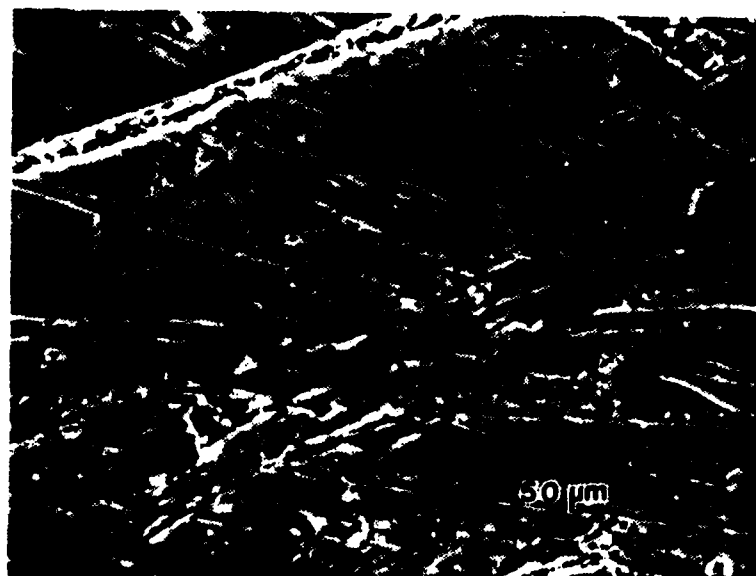


Figure 38. As Machined Surface of 304 Stainless Steel



Figure 39. Corroded Surface of 304 Stainless Steel

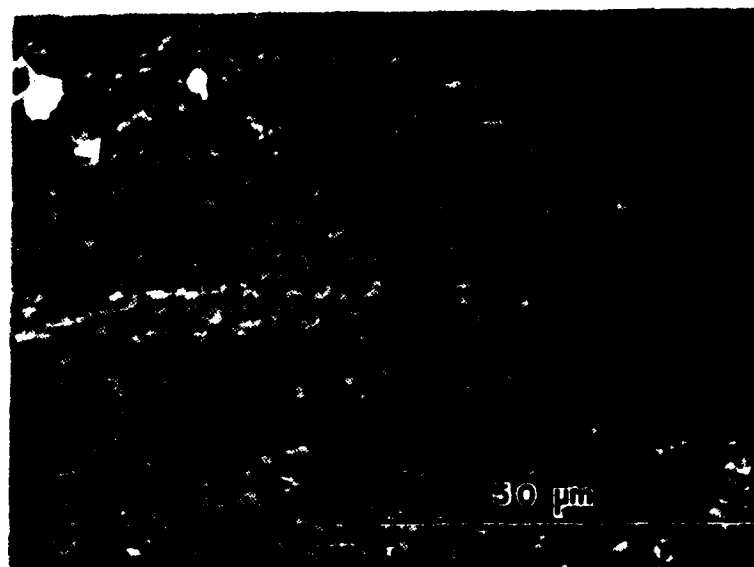


Figure 40. As Machined Surface of Cu-Mn-Al-Fe-Ni



Figure 41. Corroded Surface of Cu-Mn-Al-Fe-Ni



Figure 42. Surface Appearance of 7075 Aluminum

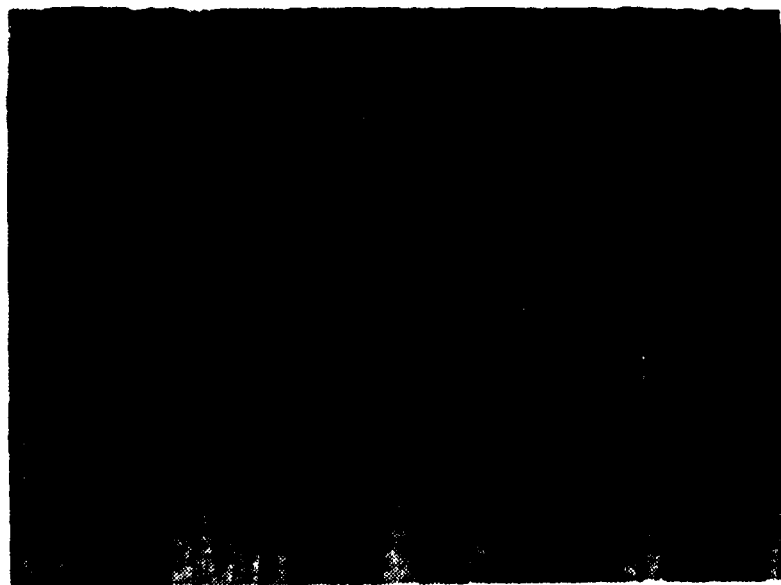


Figure 43. Surface Appearance of 630 Bronze

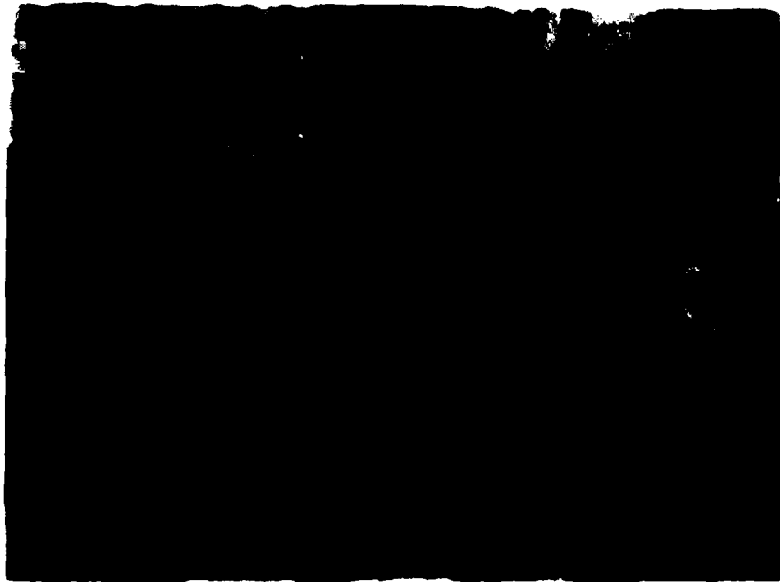


Figure 44. Surface Appearance of Fe-Cr Mo

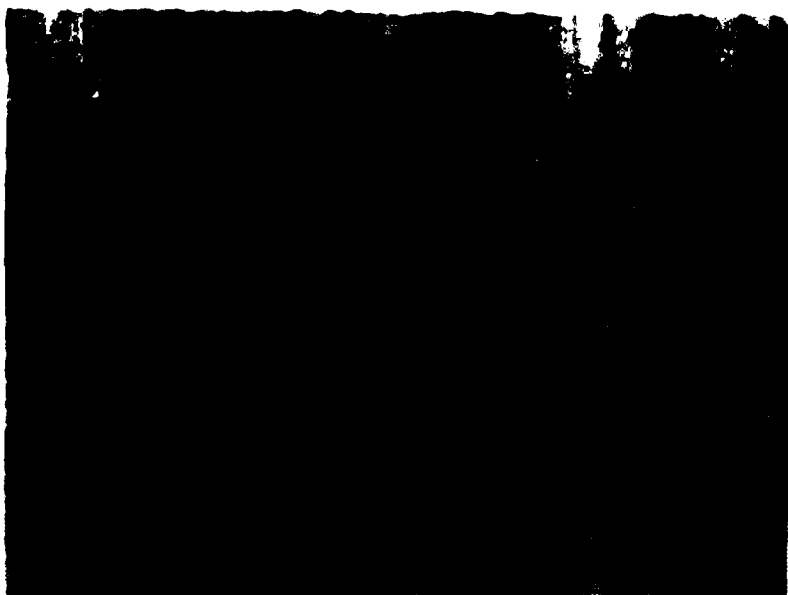


Figure 45. Surface Appearance of Fe-Cr-Al



Figure 46. Surface Appearance of Cu-Mn-Al



Figure 47. Surface Appearance of 304 Stainless Steel

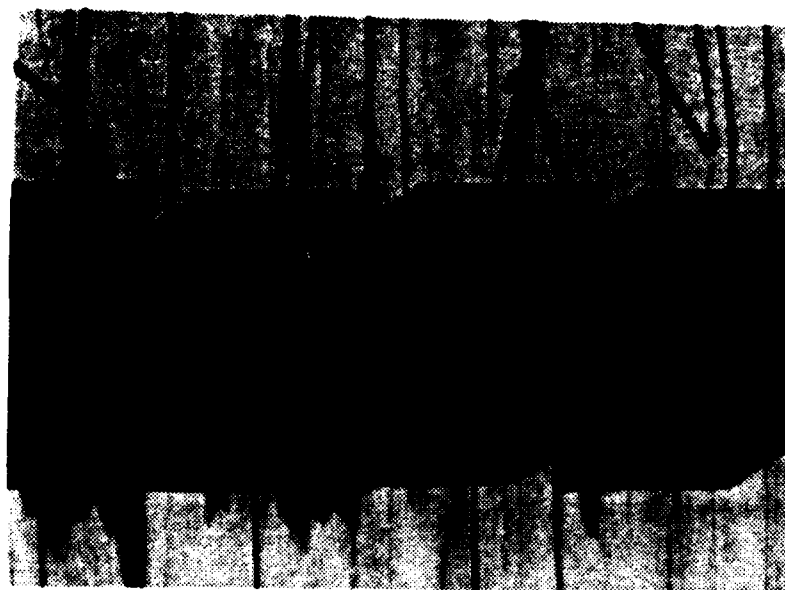


Figure 48. Surface Appearance of Cu-Mn-Al-Fe-Ni

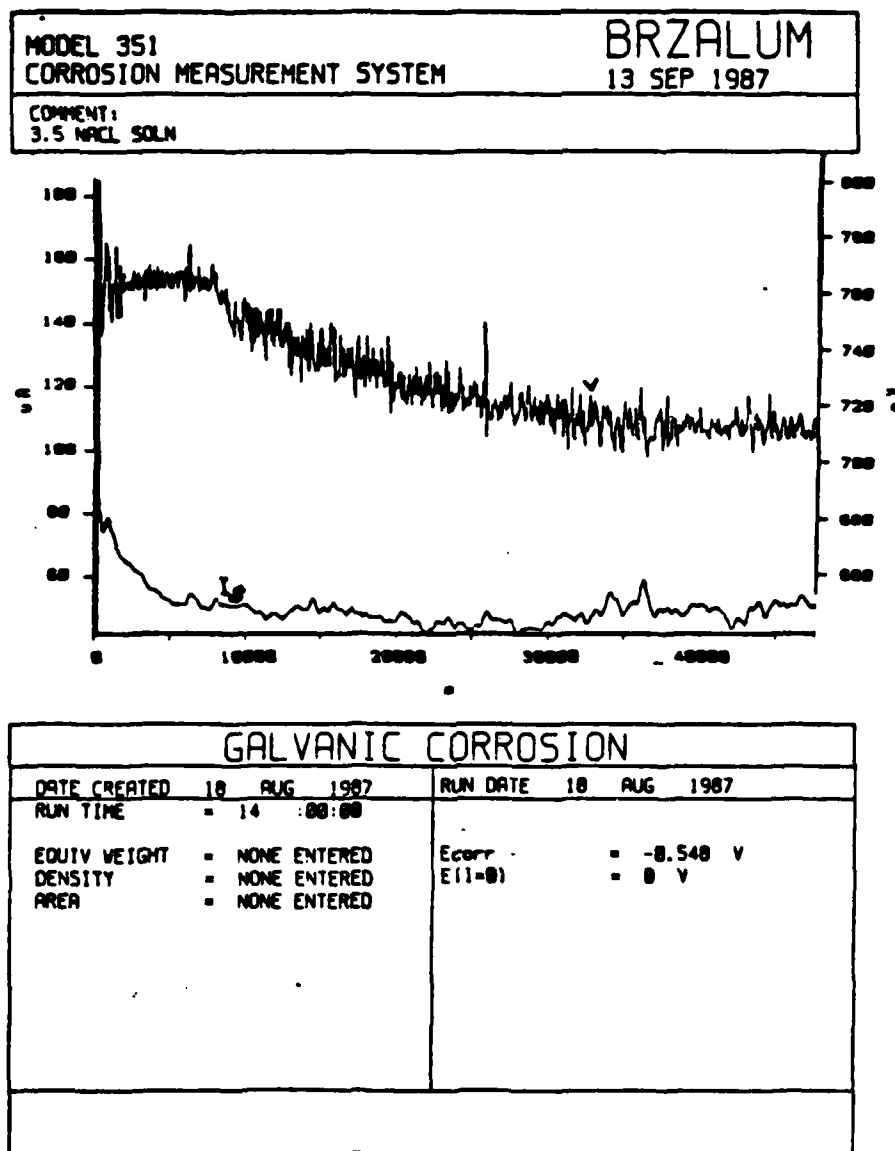


Figure 49. 7075 Aluminum Coupled with 630 Bronze

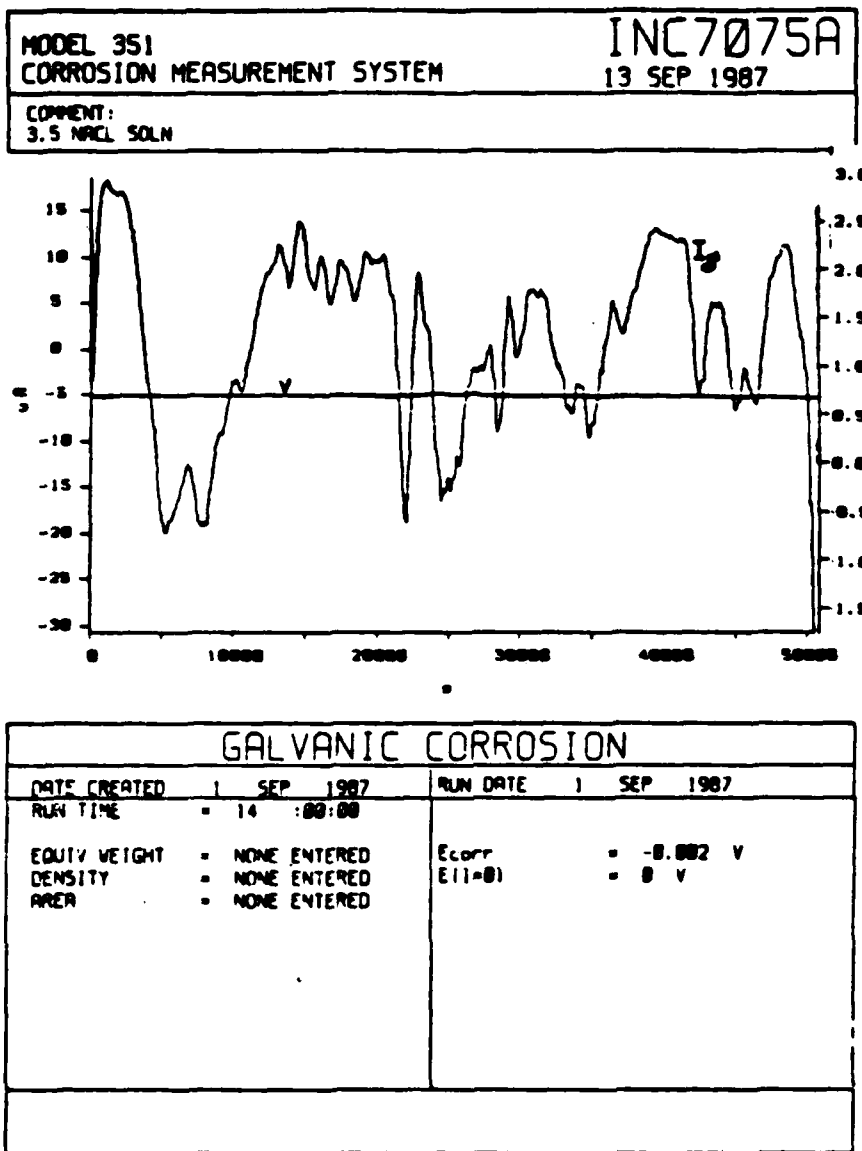
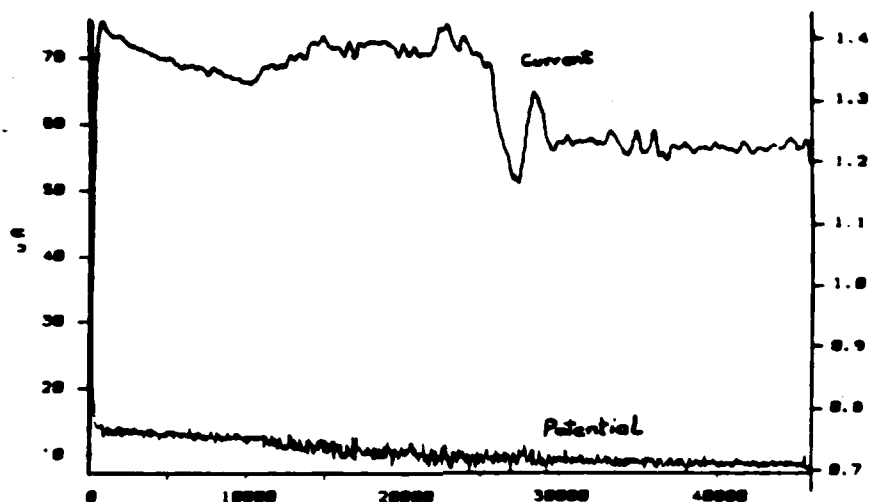


Figure 50. 7075 Aluminum Coupled with Incramute

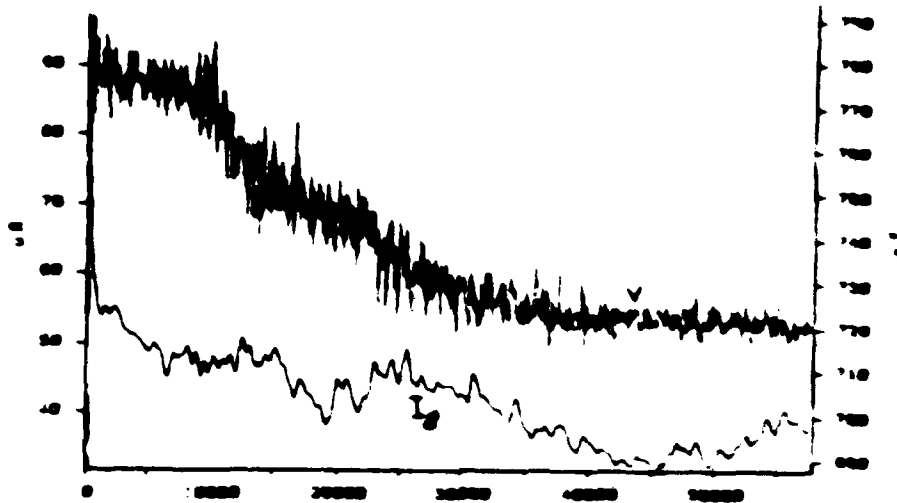
MODEL 351 CORROSION MEASUREMENT SYSTEM	SONALUM 13 SEP 1987
COMMENT: 3.5 NAACL SOLN	



GALVANIC CORROSION			
DATE CREATED	: JUL 1987	RUN DATE	: JUL 1987
RUN TIME	= 13 03.00		
EQUIV WEIGHT	= NONE ENTERED	Ecorr	= 0.005 V
DENSITY	= NONE ENTERED	E(I=0)	= 0 V
AREA	= NONE ENTERED		

Figure 51. 7075 Aluminum Coupled with Sonoston

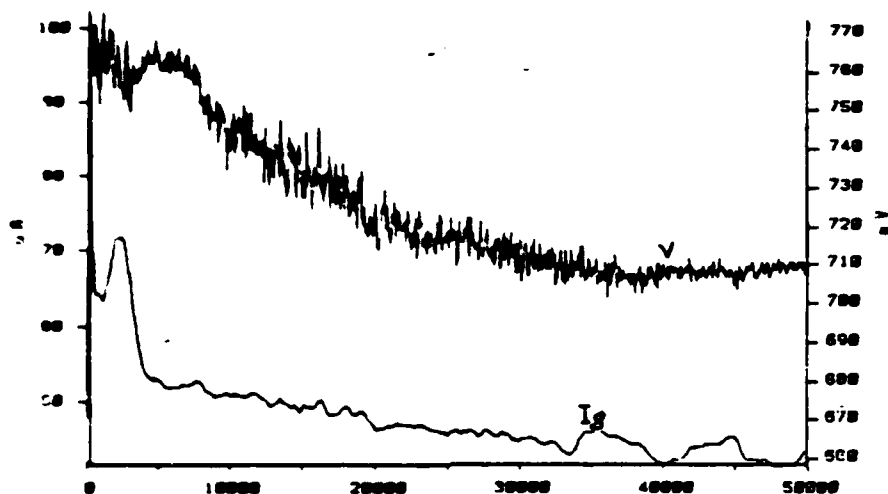
MODEL 351	VM07075A
CORROSION MEASUREMENT SYSTEM	13 SEP 1987
CURRENT 9.5 MPOL SOLN	



GALVANIC CORROSION					
DATE LAUNCH	17	AUG	1987	RUN DATE	17 AUG 1987
RUN TIME	16	00	00		
EQUIV WEIGHT	NONE ENTERED			Ecorr	-0.566 V
DENSITY	NONE ENTERED			E11-01	0 V
AREA	NONE ENTERED				

Figure 52. 7075 Aluminum Coupled with Fe-Cr-Mo

MODEL 351 CORROSION MEASUREMENT SYSTEM	ST304AL 13 SEP 1987
COMMENT: 3.5 NAACL SOLN	



GALVANIC CORROSION			
DATE CREATED	6 SEP 1987	RUN DATE	7 SEP 1987
RUN TIME	= 50000 SEC		
EQUIV WEIGHT	= NONE ENTERED	Ecorr	= -0.486 V
DENSITY	= NONE ENTERED	E(1=0)	= 0 V
AREA	= NONE ENTERED		

Figure 53. 7075 Aluminum Coupled with 304 Stainless Steel

AD-A188 848

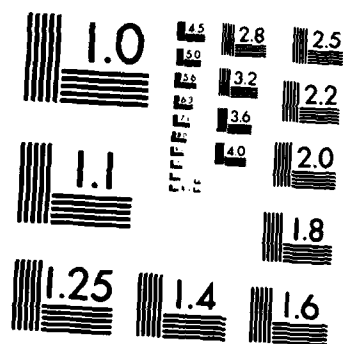
CORROSION PERFORMANCE OF HIGH DAMPING ALLOYS IN 35%
SODIUM CHLORIDE ENVIRONMENT(U) NAVAL POSTGRADUATE
SCHOOL MONTEREY CA 5 AKHTAR SEP 87

2/2

UNCLASSIFIED

F/G 11/6.1 ML





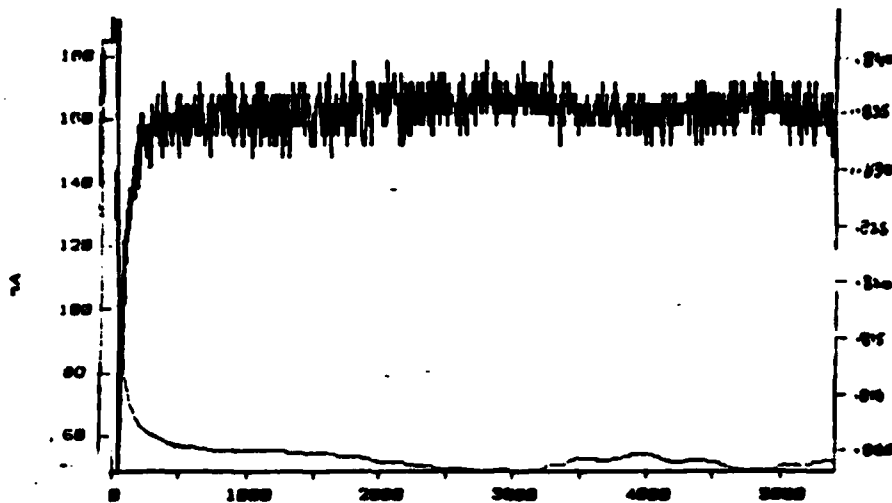
MICROCOPY RESOLUTION TEST CHART
NATIONAL BUREAU OF STANDARDS 1963-A

MODEL 351
CORROSION MEASUREMENT SYSTEM

V27075AL

17 JUL 1987

COMMENT:
3.5 NAOL SOLN

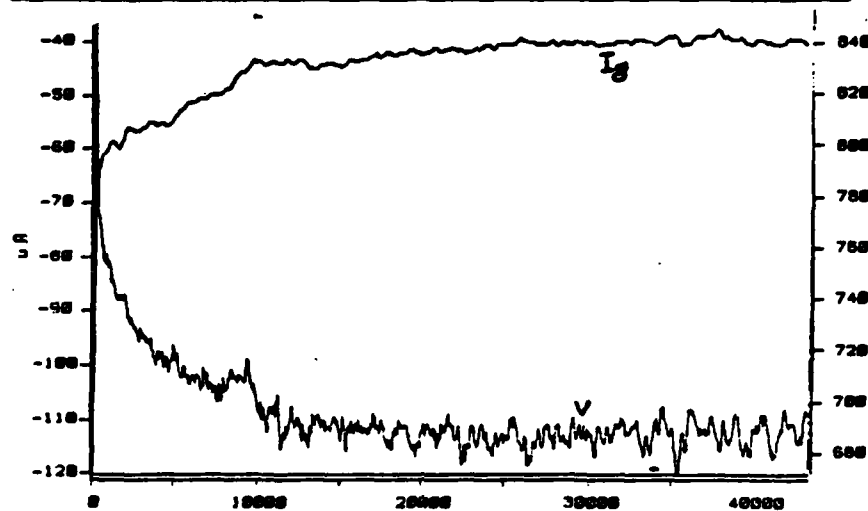


GALVANIC CORROSION

DATE CREATED	17 JUL 1987	RUN DATE	17 JUL 1987
RUN TIME	1 15:10		
EQUIV WEIGHT	8.994 g/EQUIV	E _{corr}	-0.565 V
DENSITY	2.72 g/cm ³	E(I=0)	0 V
AREA	8.283 cm ²	CORR RATE	0 MPY

Figure 54. 7075 Aluminum Coupled with Fe-Cr-Al

MODEL 351 CORROSION MEASUREMENT SYSTEM	SONO304 13 SEP 1987
COMMENT: SHIELDED-LATE NIGHT 3.5 NAOL	



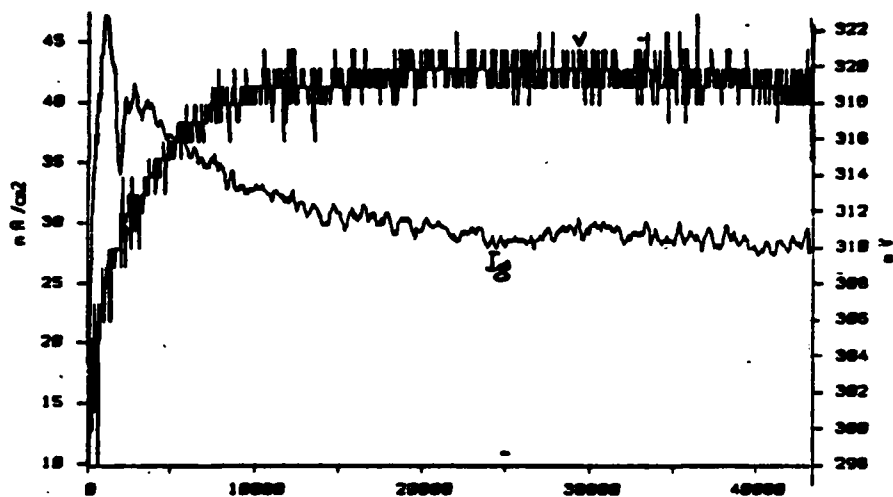
GALVANIC CORROSION					
DATE CREATED	22	JUL	1987	RUN DATE	22 JUL 1987
RUN TIME	=	12	:00:00		
EQUIV WEIGHT	=	NONE ENTERED			
DENSITY	=	NONE ENTERED			
AREA	=	NONE ENTERED			
				Ecorr	= 0.55 V
				E(I=0)	= 0 V

Figure 55. 304 Stainless Steel Coupled with Sonoston

MODEL 351
CORROSION MEASUREMENT SYSTEM

STLBRNZ
13 SEP 1987

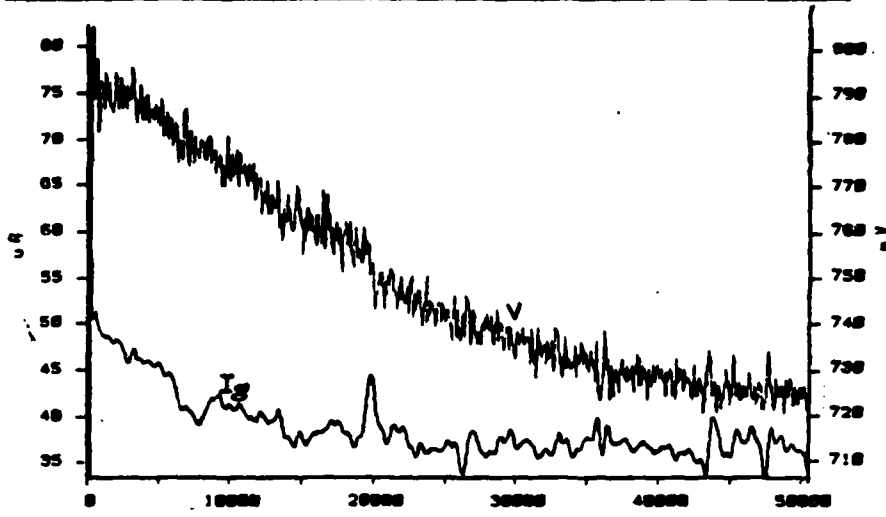
COMMENT:
3.5 NAEL SOLN GALV CORR



GALVANIC CORROSION					
DATE CREATED	19	JUL	1987	RUN DATE	19 JUL 1987
RUN TIME	= 12 :00:00				
EQUIV WEIGHT	=	27.93	g/EQUIV	Ecorr	= -0.81 V
DENSITY	=	5.423	g/cm3	E(I=0)	= 0 V
AREA	=	5.071	cm2	CORR RATE	= 0 MPY

Figure 56. 304 Stainless Steel Coupled with 630 Bronze

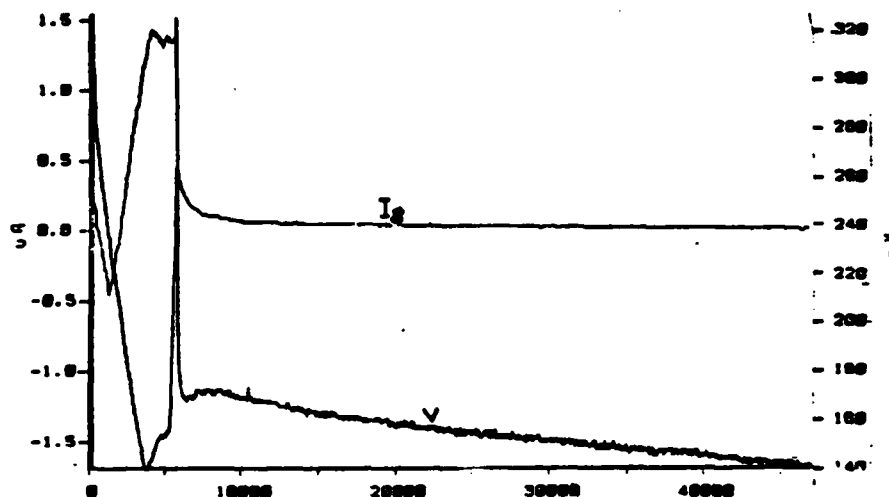
MODEL 351 CORROSION MEASUREMENT SYSTEM	INC304SS 13 SEP 1987
COMMENT: 3.5 NAACL SOLN	



GALVANIC CORROSION			
DATE CREATED	13 AUG 1987	RUN DATE	13 AUG 1987
RUN TIME	= 14 :00:00		
EQUIV WEIGHT	= NONE ENTERED	Ecorr	= -0.546 V
DENSITY	= NONE ENTERED	E[I=0]	= 0 V
AREA	= NONE ENTERED		

Figure 57. 304 Stainless Steel Coupled with Incramute

MODEL 351 CORROSION MEASUREMENT SYSTEM	V255304 13 SEP 1987
COMMENT: 3.5 NAEL SOLN	



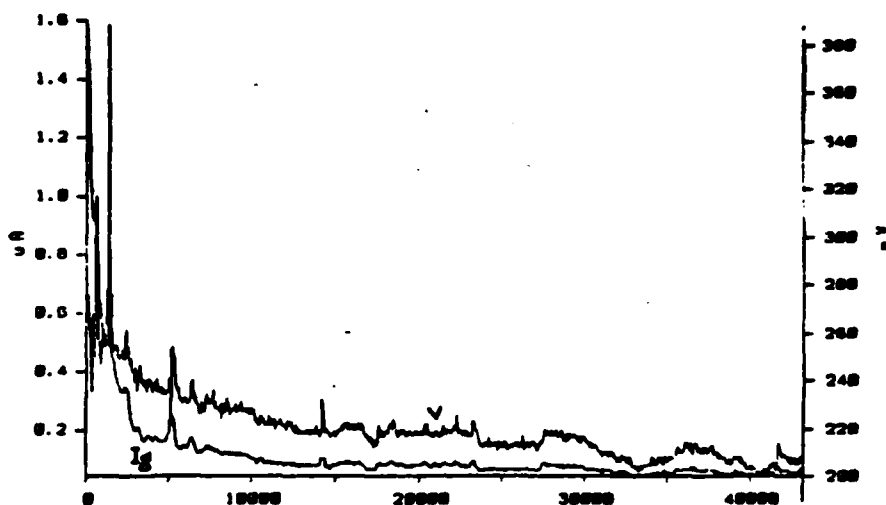
GALVANIC CORROSION			
DATE CREATED	1	AUG 1987	RUN DATE 2 AUG 1987
RUN TIME	=	13 :00:00	
EQUIV WEIGHT	=	NONE ENTERED	Ecorr = -0.87 V
DENSITY	=	NONE ENTERED	E(I=0) = 0 V
AREA	=	NONE ENTERED	

Figure 58. 304 Stainless Steel Coupled with Fe-Cr-Al

MODEL 351
CORROSION MEASUREMENT SYSTEM

VAM304SS
13 SEP 1987

COMMENT:
3.5 NACL SOLN



GALVANIC CORROSION

DATE CREATED 27 JUL 1987
RUN TIME = 12 :00:00

RUN DATE 28 JUL 1987

EQUIV WEIGHT = NONE ENTERED
DENSITY = NONE ENTERED
AREA = NONE ENTERED

Ecorr = -0.88 V
E(1-01) = 0 V

Figure 59. 304 Stainless Steel Coupled with Fe-Cr-Mo

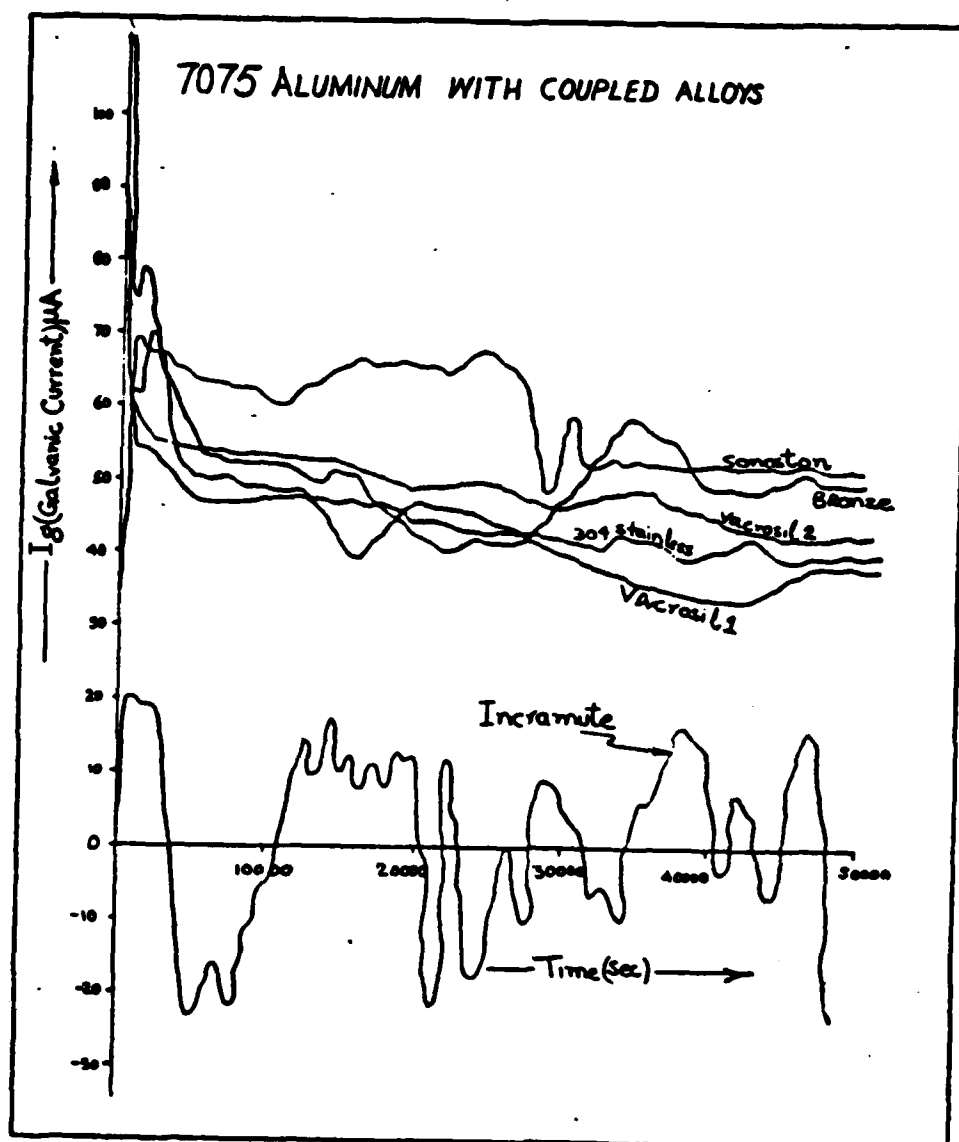


Figure 60. Coupling 7075 Aluminum with Rest of the Alloys

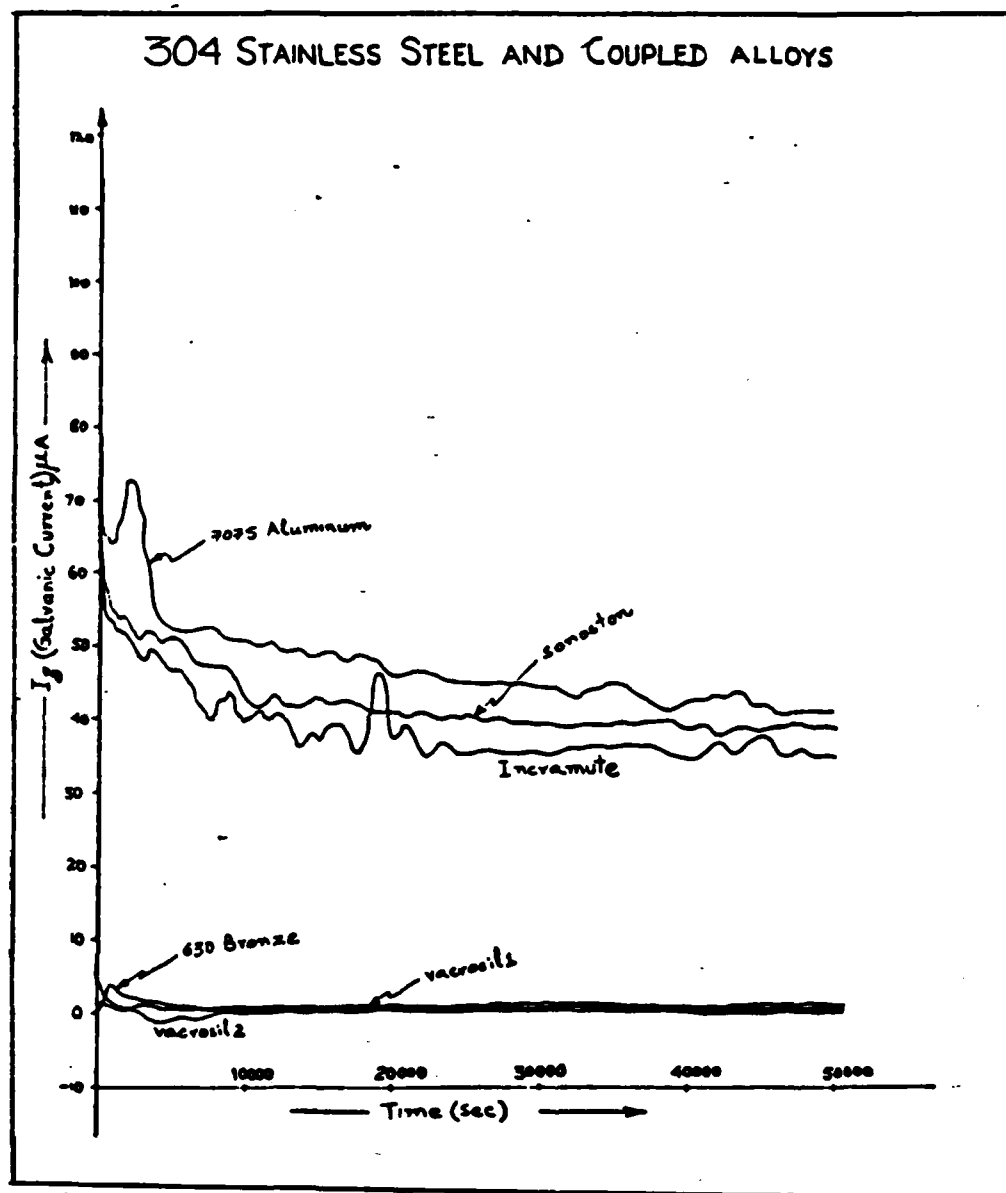


Figure 61. Coupling 304 Stainless Steel with Rest of the Alloys

TABLE 1
RESULTS OF SINGLE METAL CORROSION

ELEMENT ALLOY	E_{CORR} (Volts)	S gm/cm ³	wt	i_{CORR} (PDP) A/cm ²	i_{CORR} (LPR) A/cm ²	(PDP) mpy	(LPR) mpy	3.5% NaCl Solution (Salem) AVG (mpy)	Natural Sea water (LaQue) AVG (mpy)	Synthetic Sea water (Bacue) AVG (mpy)
7075 ALUMINUM	- 0.785	2.8	8.994	7.408	11.7	3.11	5.6	4.355	6.5	0.2955
INCONEL	- 0.779	2.58	29.59	6.0618	10.8	9.08	16.2	12.6	3.6	0.541
SONOSTON	- 0.6733	7.27	28.32	4.64	2.11	2.36	1.07	1.715	2.5	4.665
Fe-Cr-Al	- 0.370	7.2	26.15	0.6598	1.18	0.313	0.551	0.432	2.2	0.455
Fe-Cr-Mo	- 0.276	7.6	26.34	0.0403	0.613	0.018	0.276	0.147	3.3	0.677
630 BRONZE	- 0.245	7.5	27.67	0.1285	4.48	0.062	2.12	1.09	0.5	1.578
304 STAINLESS STEEL	- 0.217 (active) - 0.053 (passive)	7.9	27.93	0.1	0.02	0.05	0.0095	0.029	0.1	0.433

APPENDIX B

PREPARATION OF 3.5% SODIUM CHLORIDE SOLUTION

3.5% Sodium Chloride solution was made from Sodium Chloride Crystals which meets the ACS specifications. Maximum limits of impurities are as under:

Constituents	Percentage
Ba	0.001
Br	0.01
Cl, Mg	0.005
NO ₃	0.003
Pb	0.0005
I	0.002
Fe	0.0002
N	0.001
PO ₄	0.0005
K	0.005
SO ₄	0.004

35 grams of Sodium Chloride crystals were added for each litre of distilled water. The solution was prepared in parts of 15 litres at one time. 525 grams of Sodium

Chloride crystals were mixed separately in about 2 litres of distilled water. It was then heated slightly and stirred until fully dissolved. This was then added to main bulk of distilled water and allowed to settle for 24 hours. Any insoluble impurities were drained off from bottom of the container.

APPENDIX C

STANDARD OPERATING PROCEDURES FOR THE MODEL 351 CORROSION MEASUREMENT SYSTEM

1. Prepare the specimen and the cell in accordance with ASTM Standard G 5 - 72 and Figure . Record dimensions and weight of the sample.
2. Energize the Plotter and Potentiostat.
3. Energize the Model 1000 Processor.
4. Insert the Corrosion Operating Procedure diskette to boot-up the system.
5. The program is menu driven. Enter appropriate experimental data including time, date, etc... Insert a diskette for data collection.
6. Return to the Main Menu and choose the desired experimental technique. At this stage, previously used experimental in - puts or new operating parameters can be selected. Subtract $.2463 \text{ cm}^2$ and $.0196 \text{ cm}^3$ from the calculated surface area and volume respectively. These constants account for the loss in surface area due to the Teflon tip contact and the loss in volume due to the sample holder penetration into the specimen.
7. Once experimental parameters have been selected, assign the experiment to the corrosion cell.

8. Energize the cell Enable switch (on the Potentiostat) and run the experiment.
9. After the data collection is complete, return to the Main Menu and store the experiment.
10. At this time, the experimental display can be plotted.
11. Corrosion rates can now be calculated from the experimental results.

LIST OF REFERENCES

1. Ailor, W.H., Handbook on Corrosion Testing and Evaluation, pp. 182 - 184, John Wiley and Sons, 1975.
2. Fontana, M.G., and Staehle, R.W., Advances in Corrosion Science and Technology, v. 6, pp. 185 -189, Plenum Press, 1976.
3. Uhlig, H.H., and Revie, R.W., Corrosion and Corrosion Control, 3rd ed., pp. 53 - 56, John Wiley and Sons, 1985.
4. Pourbaix, M., Lectures on Electrochemical Corrosion, p. 252, Plenum Press, 1973.
5. Wilde, B.E., An Assembly for Electrochemical Corrosion Studies in Aqueous Environments, Corrosion, v. 23, pp. 331 - 333, November 1967.
6. National Association of Corrosion Engineers, NACE Basic Corrosion Course, pp. 1 - 15, 1975.
7. LaQue, Francis L., Marine Corrosion Causes and Prevention, pp. 148 - 150, John Wiley and Sons, 1975.
8. Sedriks, A. John, Corrosion and Stainless Steels, pp. 99 - 108, John Wiley and Sons, 1979.
9. Schumacher, M., editor, Seawater Corrosion Handbook, pp. 5 - 8, Noyes Data Corporation, 1979.
10. Baboian, R., editor, Electrochemical Techniques for Corrosion, pp. 73 - 78, NACE Publication, 1977.

11. Baboian. R., Localized Corrosion - Cause of metal failure, pp. 145 - 163, ASTM 1972.
12. Brown, R.H., and Mears, R.B., Trans. Electrochem. Society., Vol. 74, p. 510, 1983.
13. Devay, J., Lenyal, B., and Meszaros, L., Acta Chim, Hung., Vol. 62, p. 157, 1969.
14. Fraunhofer, J.A., and Staheli, P.J., Corrosion Science, Vol. 12, p. 767, 1972.

INITIAL DISTRIBUTION LIST

	No. Copies
1. Defense Technical Information Center Cameron Station Alexandria, Virginia 22304-6145	2
2. Library, Code 0142 Naval Postgraduate School Monterey, California 93943-5002	2
3. Department Chairman, Code 69Hy Department of Mechanical Engineering Naval Postgraduate School Monterey, California 93943-5000	1
4. Professor A.J. Perkins, Code 69Ps Department of Mechanical Engineering Naval Postgraduate School Monterey, California 93943-5000	8
5. Mr. A.G.S. Morton, Code 2813 David W. Taylor Naval Ship R & D Center Annapolis, Maryland 21402	5
6. LCDR Saleem Akhtar, Pakistan Navy B-68, Block II, Gulshan-e-Iqbal Karachi, Pakistan	3
7. Commander Logistics c/o F.M.O. PN Dockyard Karachi, Pakistan	1
8. Assistant Chief of Naval Staff (Tech) Naval Headquarter Islamabad, Pakistan	1
9. Director Ships Maintenance and Repairs Naval Headquarter Islamabad, Pakistan	1
10. General Manager Dockyard c/o F.M.O., PN Dockyard Karachi, Pakistan	1
11. Director Naval Training Naval Headquarter Islamabad, Pakistan	1

- | | |
|--|---|
| 12. Director Naval Construction
Naval Headquarter
Islamabad, Pakistan | 1 |
| 13. Commanding Officer
Pakistan Naval Engineering College
PNS JAUHAR
c/o Fleet Mail Office
Karachi, Pakistan | 2 |
| 14. Commanding Officer
PNS Karsaz
Shahrai-e-Faisal
Karachi, Pakistan | 1 |

END
FILMED
FEB. 1988
DTIC